THEORETICAL INVESTIGATION OF STANDING WAVES IN HYDRAULIC STRUCTURES

By

ARCHIE ALLAN STONE

Massachusetts Institute of Technology

September, 1946

✓

Cambridge, Massachusetts

September 16, 1946

This thesis is respectfully submitted in partial fulfillment of the requirements for the degree of Master of Science.

Archie Allan Stone

Approved and accepted in partial fulfillment of the requirements for the degree of Master of Science.

Date

The author wishes to state his grateful appreciation of the help of Dr. Arthur T. Ippen, associate professor of hydraulics at the Massachusetts Institute of Technology, at whose suggestion and under whose guidance this study was undertaken.

Dr. Ippen's broad experience and extensive work in the field of supercritical flow in hydraulic structures has made him one of the outstanding engineers in this field. It has been a privilege and a very valuable experience to work with him.

TABLE OF CONTENTS

TABLE OF CONTENTS cont.

ILLUSTRATIONS

ILLUSTRATIONS cont.

ILLUSTRATIONS cont.

INTRODUCTION

NATURE OF THE PROBLEM

The recent upswing in the development of natural hydraulic resources in this country and abroad has resulted in the design of many power, irrigation and flood control projects in which high velocities of flow are utilized for the rapid and efficient handling of water.

This high velocity flow has introduced problems in hydraulic engineering which had not previously been encountered. Chief among these problems is the formation of standing waves, which are usually unpredictable and require expensive high-walled structures to prevent overtopping.

Methods of design used in the analysis of low velocity structures have been found insufficient and cannot be utiliz ed to predict standing wave formation. Many high velocity channels have of course been designed, and with some degree of success. But these channels were designed by empirical methods without making any contribution to our understanding of the fundamental factors which underlie the problem.

Recently, i.e. in the last ten or fifteen years, some research has been done on the subject of high velocity flow in channels with a free surface. Most

important of this work has followed from the recognition of the analogy between supercritical flow

Figure 1

Standing Waves in Laboratory Apparatus

in water and supersonic flow in gases. This analogy has made possible the utilization in hydraulic design of methods which have been highly developed in gas dynamics.

Supersonic flow in gases occurs when the velocity of flow is greater than the local velocity of a compression wave. Since sound travels at the velocity of a compression wave, or more correctly, since sound is a compression wave, such flow is termed supersonic.

Supercritical flow in water occurs when the velocity of flow is greater than the velocity of a small wave disturbance in the water surface. This velocity, termed the critical velocity, is given by the equation:

$$V_c = \sqrt{gh}$$

where h is the water depth.

Hereafter in this thesis supercritical flow will signify that $V > V_c$, subcritical flow that $V < V_c$.

HISTORICAL NOTE:

The analogy between supercritical flow in water and supersonic flow in gases was pointed out by Prandtl in 1931. (See reference 1 in bibliography) It has received thorough mathematical treatment by Prandtl, Von Karman (2), Riabouchinsky (3), and Busemann (4). Their work was extended and verified by Preiswerk (5), whose published report of

his theoretical and experimental study, based on the methods of gas dynamics, of flow in the Laval nozzle is especially noteworthy as an example of the methods of design based on gas wave theory.

In this country, Ippen and Knapp (6) did further research on this subject, and Ippen (7) has published a very concise summary of the previous work, demonstrating in some detail the methods involved in hydraulic design.

PURPOSE AND SCOPE OF THIS WORK:

The purpose of this thesis is to demonstrate the correlation between theory based on the methods of gas dynamics and experimental results obtained in laboratory flumes. A study is made of two types of channel contractions at various velocities of flow in the supercritical range.

THEORY

THE STANDING WAVE

If the velocity of a wave with respect to the body of water on which it moves is C, usually called the wave celerity, the wave when propagated by a point source of disturbance will move out in all directions at the velocity C, and at any time T the wave front will form a circle of radius CT.

If the wave is propagated on the surface of water which is moving down a channel with velocity V, the center of the wave front will move downstream with the velocity V. At any time T after the wave is propagated the center will be a distance VT downstream from the disturbance source, and the wave front will still be a circle of radius CT.

The velocity with which the disturbance moves directly upstream is then given by C - V, and the velocity with which it moves directly downstream is given by C + V. Thus if V is greater than C, the disturbance is never transmitted upstream. When V is greater than C the flow is termed supercritical, and the consequence that in supercritical flow disturbances are not transmitted upstream is of considerable importance in hydraulic design.

We may now investigate the manner in which a standing wave is formed in supercritical flow. A standing wave is a stationary wave, a wave which does not move with respect to a stationary observer. In other words its velocity with respect to the water over which it moves is equal and opposite to the absolute velocity of the water. Assume that the source of disturbance is a change in wall angle θ, (Figure 2). The water is flowing with a velocity V which we assume to be greater than the wave velocity C.

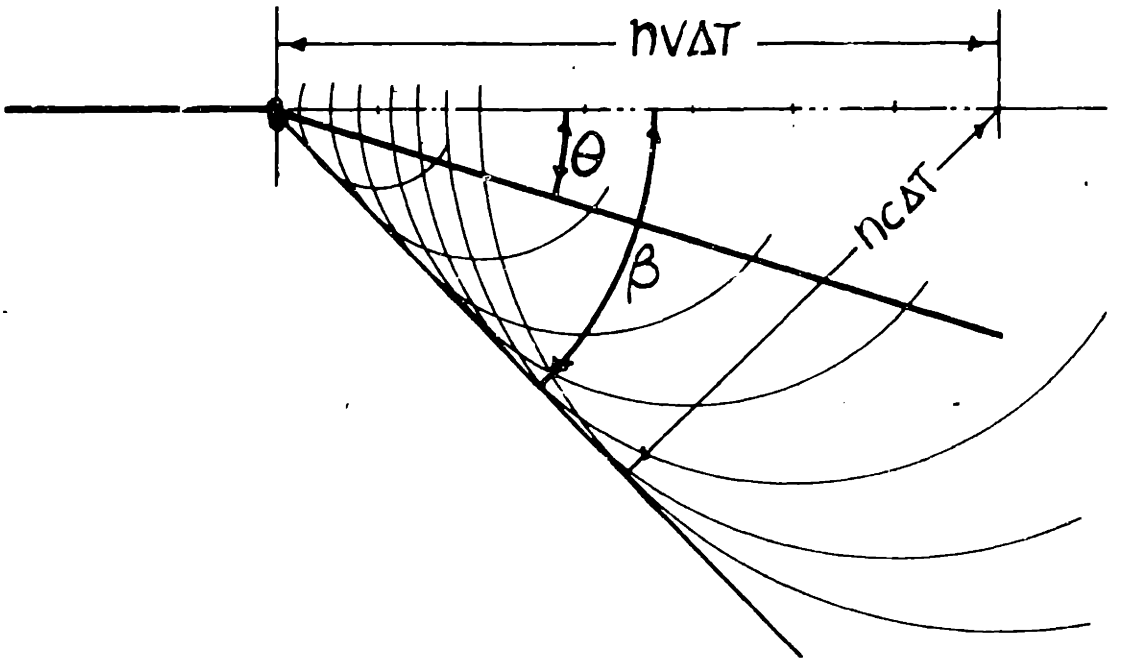

Figure 2

The disturbance is continuous, that is new disturbance waves are constantly being propagated.

We shall study the disturbances which are propagated at small intervals of time ΔT.

After an interval of time $n\Delta T$ since its propagation, the center of a wave front will have moved downstream a distance $nV\Delta T$ from the disturbance source. In this time the radius of the wave front has increased to $nC\Delta T$. The angle β between the original velocity vector and the tangent to the wave front through the disturbance source is given by:

$$\sin\beta = \frac{nC\Delta T}{nV\Delta T} = \frac{C}{V}$$

This equation shows that the angle β is independent of time, and is a property of all the waves originating at the disturbance source. Hence all of these waves have a common tangent passing through the disturbance source, and this tangent is the limit above which the disturbance is not transmitted. This tangent is then a standing wave front.

DERIVATION OF WAVE CELERITY - C

We may now proceed to determine the factors which determine the angle β. We have found that $\sin\beta = \frac{C}{V}$. V is a measurable quantity, predetermined for a given design. We shall determine C as follows. Referring to figure 3, we have a flow which is sub-

ject to a disturbance such that the stream lines are deflected through an angle θ as the flow crosses

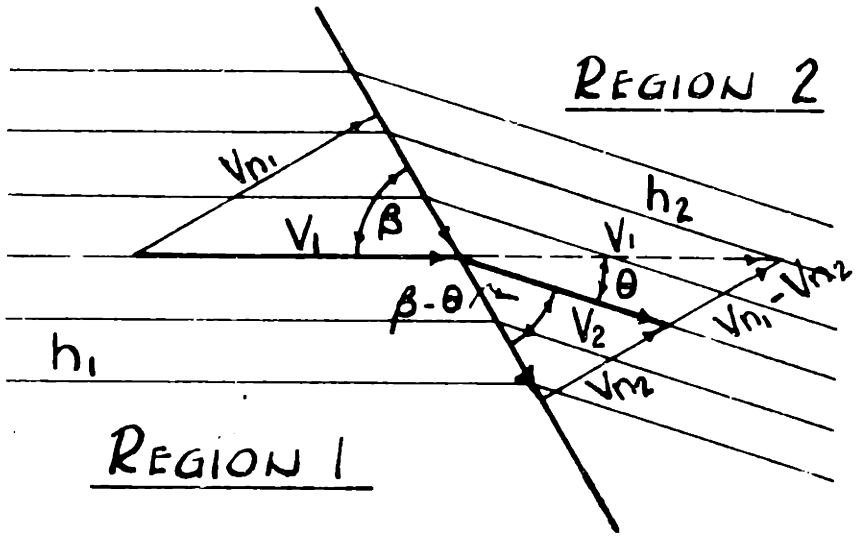

Figure 3

the standing wave shown. In region 1, the depth is h_1, the velocity is V_1, with components normal and tangential to the wave front given by V_{n1} and V_{t1} respectively. Beyond the wave front in region 2 we have h_2, V_2, V_{n2}, and the same tangential component V_{t1}.

From continuity considerations we may write:

$$h_1 V_{n1} = h_2 V_{n2}.$$

Whence:

$$V_{n2} = \frac{h_1}{h_2} V_{n1} \tag{1}$$

From the geometry of the flow:

$$V_{n1} = V_1 \sin\beta = C \tag{2}$$

The above follows from the fact that V_{n1} is the velocity of the approaching water relative to the wave front and vice versa.

From the momentum equation:

The static force across the wave front per unit length of wave is given by:

$$\frac{1}{2} w h_2^2 - \frac{1}{2} w h_1^2 = \frac{w}{2} (h_2^2 - h_1^2) \tag{3}$$

The change in momentum across the wave front per unit length of wave is given by:

$$\frac{w}{g} V_{n1} h_1 (V_{n1} - V_{n2}) \tag{4}$$

Substituting from (1), (4) becomes:

$$\frac{w}{g} V_{n1}^2 h_1 \left(1 - \frac{h_1}{h_2}\right) = \frac{w}{g} V_{n1}^2 \frac{h_1}{h_2} (h_2 - h_1) \tag{5}$$

Equating (3) and (5):

$$\frac{w}{2} (h_2^2 - h_1^2) = \frac{w}{g} V_{n1}^2 \frac{h_1}{h_2} (h_2 - h_1)$$

Solving for V_{n1}^2:

$$V_{n1}^2 = \frac{g}{2} \frac{h_2}{h_1} (h_2 + h_1) = g h_1 \frac{1}{2} \frac{h_2}{h_1} \left(1 + \frac{h_2}{h_1}\right)$$

$$V_{n1} = C = \sqrt{g h_1 \frac{h_2}{h_1} \left(1 + \frac{h_2}{h_1}\right)} \tag{6}$$

We can now see that if the wave is small, i.e. if h_2/h_1 is near unity, C is approximately $\sqrt{gh_1}$, as originally stated.

DEVELOPMENT OF FLOW DIFFERENTIAL EQUATION

We are now in a position to develop an expression containing all the principal variables which affect the flow, making only such simplifying assumptions as are necessary for the mathematical analysis of the problem, without compromising seriously the accuracy of the method.

From (6) and the fact that $V_{n1} = V_1 \sin\beta$, we may write:

$$\sin\beta = \frac{\sqrt{gh_1}}{V_1}\sqrt{\frac{1}{2}\frac{h_2}{h_1}\left(1+\frac{h_2}{h_1}\right)}$$

Introducing the Froude number $F = \frac{V}{\sqrt{gh}}$, this becomes:

$$\sin\beta = \frac{1}{F_1}\sqrt{\frac{1}{2}\frac{h_2}{h_1}\left(1+\frac{h_2}{h_1}\right)} \qquad (7)$$

We have not yet introduced the angle θ, and its effect on the flow. From the geometry of the flow:

$$\frac{V_{n1}}{\tan\beta} = \frac{V_{n2}}{\tan(\beta-\theta)} = \frac{V_{n1}\frac{h_2}{h_1}}{\tan(\beta-\theta)}$$

Whence:

$$\frac{h_1}{h_2}\tan\beta - \tan(\beta-\theta) = \frac{\tan\beta-\tan\theta}{1+\tan\beta\tan\theta}$$

Solving for Tan θ:

$$\tan\theta = \frac{\tan\beta\left(1-\frac{h_1}{h_2}\right)}{1+\frac{h_1}{h_2}\tan^2\beta} \qquad (8)$$

All the above equations hold regardless of energy dissipation. We may now simplify (8) and obtain the differential equation we seek. We will make

the simplifying assumption that there is zero energy dissipation as the flow crosses a disturbance wave. To investigate the validity of this assumption, we shall determine the factors which control the amount of energy dissipation.

The energy per pound of fluid in region 1, taken with respect to the channel bottom as a datum is given by:

$$H_1 = \frac{V_1^2}{2g} + h_1$$

and the energy per pound in region 2 is given by:

$$H_2 = \frac{V_2^2}{2g} + h_2$$

The loss in energy in crossing the wave front, if the channel bottom is level, or nearly so, is:

$$\Delta H = \frac{V_1^2 - V_2^2}{2g} + (h_1 - h_2)$$

Since:

$$V_1^2 = V_{n1}^2 + V_{T1}^2 \qquad V_2^2 = V_{n2}^2 + V_{T1}^2$$

It follows that:

$$V_1^2 - V_2^2 = V_{n1}^2 - V_{n2}^2 = V_{n1}^2\left[1 - \left(\frac{h_1}{h_2}\right)^2\right]$$

From (6):

$$V_{n1}^2 = \frac{gh_1}{2}\,\frac{h_2}{h_1}\left(1 + \frac{h_2}{h_1}\right)$$

Hence:

$$V_1^2 - V_2^2 = \frac{gh_1}{2} \cdot \frac{h_2}{h_1} \cdot \left(1 + \frac{h_2}{h_1}\right) \cdot \left[1 - \left(\frac{h_1}{h_2}\right)^2\right]$$

And the lost energy per pound referred to the initial depth is given by:

$$\frac{\Delta H}{h_1} = \frac{1}{4}\frac{h_2}{h_1}\left(1+\frac{h_2}{h_1}\right)\left[1-\left(\frac{h_1}{h_2}\right)^2\right] + \frac{1}{h_1}\left(h_1 - h_2\right)$$

Multiplying out all terms in the numerator after multiplying and dividing by 4 h_2/h_1:

$$\frac{\Delta H}{h_1} = \frac{\left(\frac{h_2}{h_1}\right)^3 - 3\left(\frac{h_2}{h_1}\right)^2 + 3\frac{h_2}{h_1} - 1}{4\frac{h_2}{h_1}}$$

This is readily recognized as:

$$\frac{\Delta H}{h} = \frac{\left(\frac{h_2}{h_1} - 1\right)^3}{4\frac{h_2}{h_1}} \qquad (9)$$

It is now evident that the loss of energy is nearly zero when the wave is small, i.e. when h_2/h_1 is near unity. It is evident from (8) that this requires a small change in wall angle θ. If the change in wall angle is small:

$$TAN\,\theta \cong \theta = d\theta$$
$$h_2 - h_1 = dh$$
$$SIN\,\beta \longrightarrow \frac{1}{F}$$
$$h_1 \longrightarrow h_2 \longrightarrow h$$

Making these assumptions, we may rewrite (8) as follows:

$$TAN\,\theta = d\theta = \frac{\frac{h_2 - h_1}{h_2}TAN\,\beta}{\frac{h_2 + h_1\,TAN^2\beta}{h_2}} = \frac{dh\,TAN\,\beta}{h(1+TAN^2\beta)} = \frac{dh}{h\,csc^2\beta\,TAN\beta}$$

$$= \frac{dh}{hF^2\,TAN\beta} = \frac{dh}{\frac{V^2}{g}\,TAN\,\beta} \qquad (10)$$

THE METHOD OF CHARACTERISTICS

Equation (10) is the basis for the method of characteristics long used in gas dynamics for the solution of problems involving supersonic flow. It is this equation which demonstrates the analogy between gas and water flow. We can put it in more useful form by transforming the velocity to a dimensionless form such as $\bar{V} = \frac{V}{\sqrt{2gH}}$, WHERE H is the energy per pound of fluid with respect to the channel bottom, given by:

$$H = \frac{V^2}{2g} + h$$

Then:

$$h = H - \frac{V^2}{2g} = H\left(1 - \bar{V}^2\right)$$

$$dh = 2\bar{V}H\,d\bar{V}$$

$$\tan\beta = \frac{V_n}{V_T} = \frac{\sqrt{gh}}{\sqrt{V^2 - gh}} = \frac{\sqrt{gH(1-\bar{V}^2)}}{\sqrt{\bar{V}^2 2gH - gh(1-\bar{V}^2)}}$$

$$= \frac{\sqrt{1-\bar{V}^2}}{\sqrt{3\bar{V}^2 - 1}}$$

We may then write:

$$d\theta = \frac{2H\bar{V}\,d\bar{V}}{\bar{V}^2 \times 2H \dfrac{\sqrt{1-\bar{V}^2}}{\sqrt{3\bar{V}^2-1}}}$$

and by rearranging we obtain the equation:

$$\frac{1}{\bar{V}} \frac{d\bar{V}}{d\theta} = \frac{\sqrt{1-\bar{V}^2}}{\sqrt{3\bar{V}^2-1}} \qquad (11)$$

This expression is the differential equation in polar form of a family of epicycloids between circles of radius $\frac{1}{\sqrt{3}}$ and 1. The equation states that if the fluid is moving with a given velocity $\bar{V}$, represented in magnitude and direction by a radius vector to a point on the epicycloid, and the flow is deflected through a small angle 0, the velocity vector will be rotated through an angle 0, its point remaining on the epicycloid.

A portion of this family of epicycloids has been plotted by the author in figure 4, for angular increments of two degrees. The graphical method used with the epicycloids, called the methods of characteristics is excellently described in Dr. Ippen's paper, "Gas Wave Analogies in Open Channel Flow." (7) It is the method based on these curves which was used throughout the investigations carried out in this thesis.

POLAR CURVES - FLOW WITH ENERGY DISSIPATION

If we have flow conditions such that the flow is deflected through large angles, under which conditions

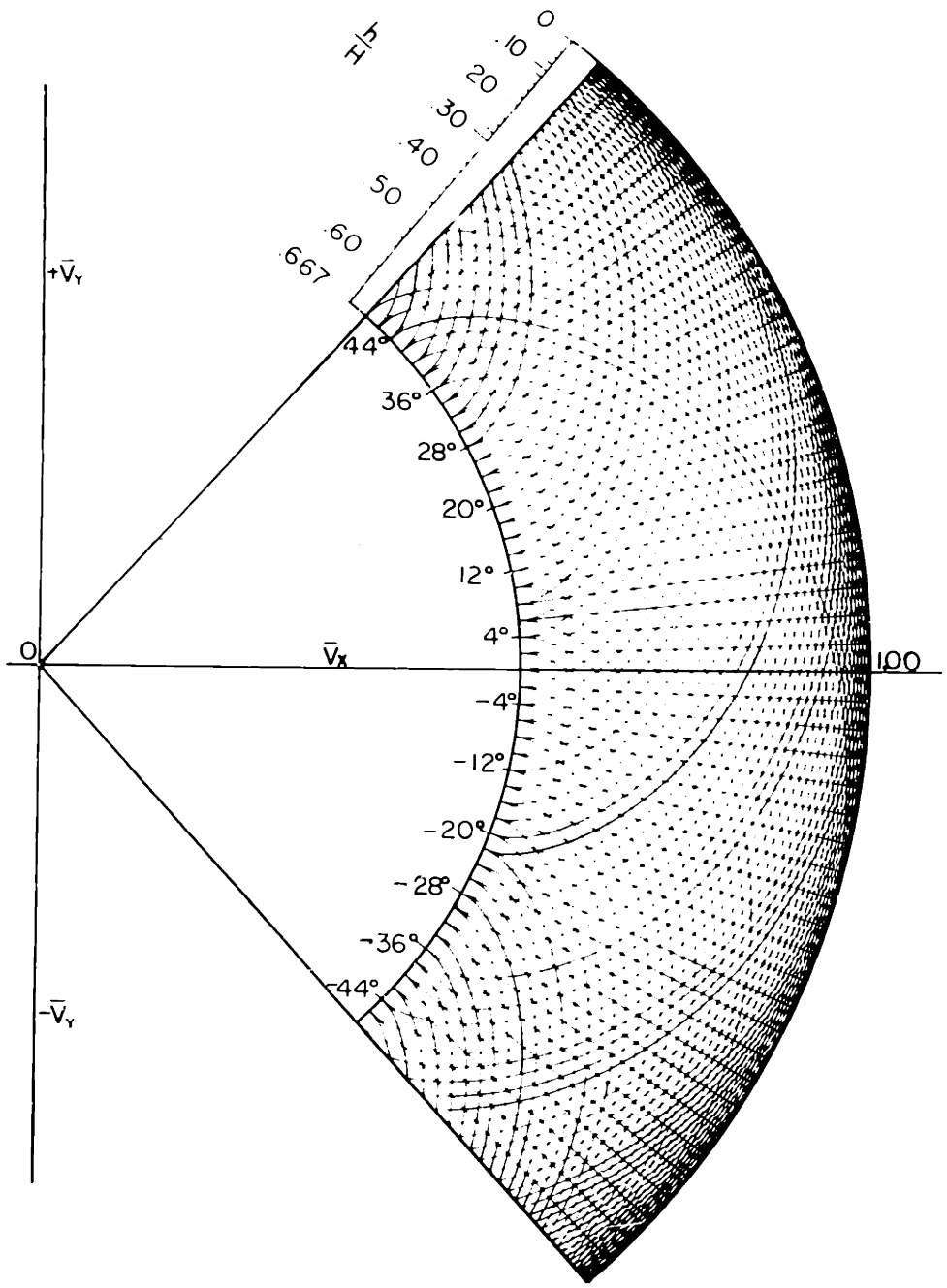

CHARACTERISTICS DIAGRAM

FIGURE 4

the assumptions underlying the method of characteristics are no longer valid, we may derive another graphical method which does not depend upon these assumptions, and in which it is not necessary to assume energy dissipation equal to zero.

If we transform equations (1) and (2) to contain the x and y components of the velocity instead of the tangential and normal components, by introduceing into these equations the geometric relationships:

$$\bar{V}_{n1}(\bar{V}_{n1} - \bar{V}_{n2}) = \bar{V}_{x1}(\bar{V}_{x1} - \bar{V}_{x2}) \qquad (12)$$

$$(\bar{V}_{n1} - \bar{V}_{n2})^2 = \bar{V}_y^2 + (\bar{V}_{x1} - \bar{V}_{x2})^2 \qquad (13)$$

we may combine the resulting expressions with the energy equation to obtain the "Jump Polar" or "Shock Polar" curves, given by the expression:

$$\bar{V}_Y^2 = \bar{V}_{x1}^2\left(1 - \frac{\bar{V}_{x2}}{\bar{V}_{x1}}\right)\left[\frac{\bar{V}_{x2}}{\bar{V}_{x1}} - \frac{\sqrt{1-\bar{V}_{x1}^2}}{\sqrt{1-\bar{V}_{x1}^2 - 4V_{x1}^2\left(1-\frac{\bar{V}_{x2}}{\bar{V}_{x1}}\right)}}\right] \qquad (14)$$

In this case, since there is energy dissipation along the channel, H is not a constant and the dimensionless velocity $\underline{\bar{V}}$ must be recomputed when each new region of the flow is reached. These curves are plotted in figure 5 and the values required for plotting the curves are given in table II in the appendix.

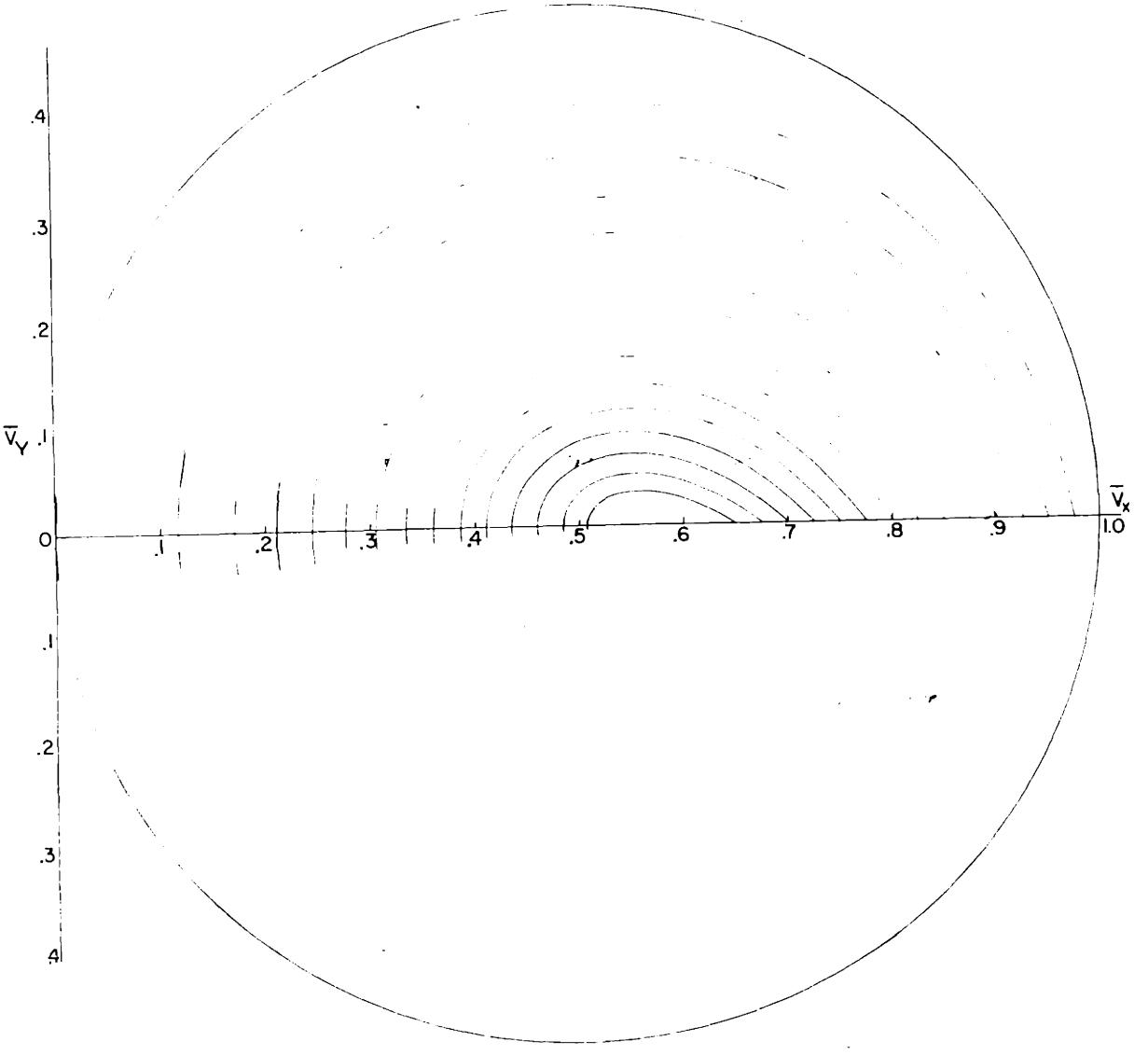

POLAR DIAGRAM FOR SLANTING HYDRAULIC JUMP

Figure 5

METHOD OF APPROACH

SOURCE OF EXPERIMENTAL DATA

The subject of this study is the correlation of experimental data with the theoretidal method previously outlined. Experimental data were available from the work of J. H. Dawson (8), D. P. Rodriguez (9), and D. Coles and T. Shintaku (10). Their work was done in the hydraulic laboratories of the University of Lehigh, under the direction of Dr. A. T. Ippen.

RESUME OF THE COLES - SHINTAKU EXPERIMENTS

Mention will first be made of the work of Coles and Shintaku, since their study brings out an important point not evident in the author's results.

These investigators, in a thesis entitled "Experimental relation between standing waves and sudden wall angle changes in supercritical flow," ran tests on the sharp angle contraction shown in figure 6, varying slope and discharge to obtain a wide range of Froude numbers. They then made measurements of the wave angle β and the depth ratio across the wave, h_2/h_1. These values were then compared in a tabulation to the theoretical values of these variables obtained from equations (7) and (8) of this work. In order to demonstrate this correlation the author

has plotted the curves of depth ratio and β thus obtained, (figure 7).

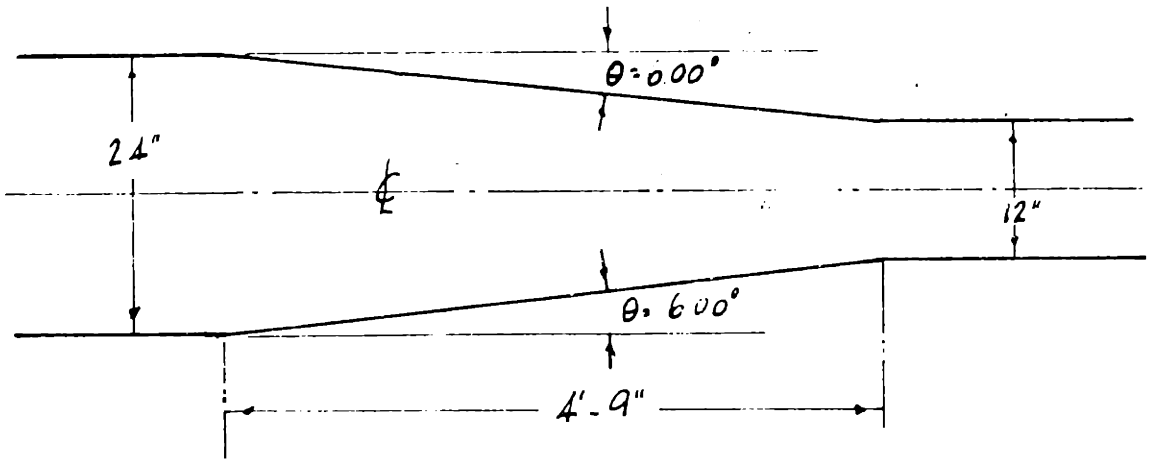

Figure 6

Coles - Shintaku channel

The tests performed by Coles and Shintaku are not numerous enough to be conclusive, but they show a definite trend. Theory and experiment show remarkable agreement between Froude numbers of 3.5 to 7.0. The theoretical and experimental curves diverge above and below this range.

This divergence is probably explained in the low Froude number range by the fact that viscous forces play a large part at low velocities, and give rise to a velocity distribution across the channel which invalidates the assumption of constant H.

COMPARISON OF EXPERIMENTAL AND CALCULATED VALUES OF h_2/h_1 AND β

(FROM WORK OF COLES AND SHINTAKU)

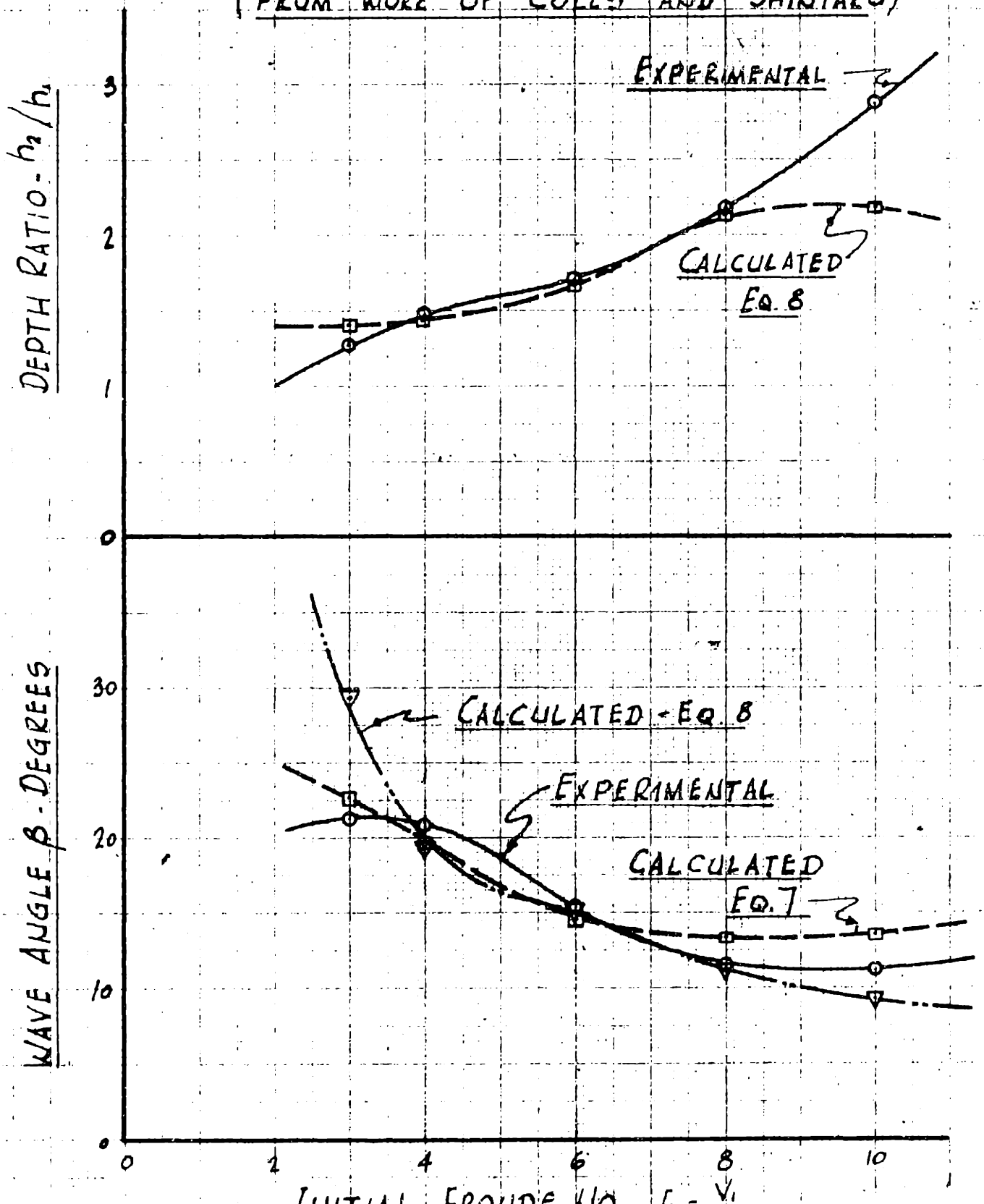

FIGURE 7

At high Froude numbers, vertical accelerations which result in non-hydrostatic pressure distributions probably cause the divergence between theory and experiment. Hydrostatic pressure distribution is a necessary condition for the validity of the statement that energy per pound $H = \frac{V^2}{2g} + h$.

Thus it would seem that theory gives the best results in the Froude number range between 3.5 and 7.0, a range in which viscous effect is relatively small and the pressure distribution in curvilinear flow is close to hydrostatic.

DAWSON EXPERIMENTS

J. H. Dawson (8) did very extensive work on the effect of lateral contractions on supercritical flow. His results for a flow with a Froude number of 4 for the symmetrical curved contraction shown in figure 8 were checked by the method of characteristics. Figure 10 shows the characteristics diagram of the flow. In figure 11 are plotted the experimental and theoretical side wall profiles which result from the contraction of the flow. The graphical construction of the flow is shown in figure 12.

RODRIGUEZ EXPERIMENTS

D. P. Rodriguez carried on experimental work using the sharp angle contraction shown in figure

9. The author made theoretical solutions by the method of characteristics for conditions corresponding

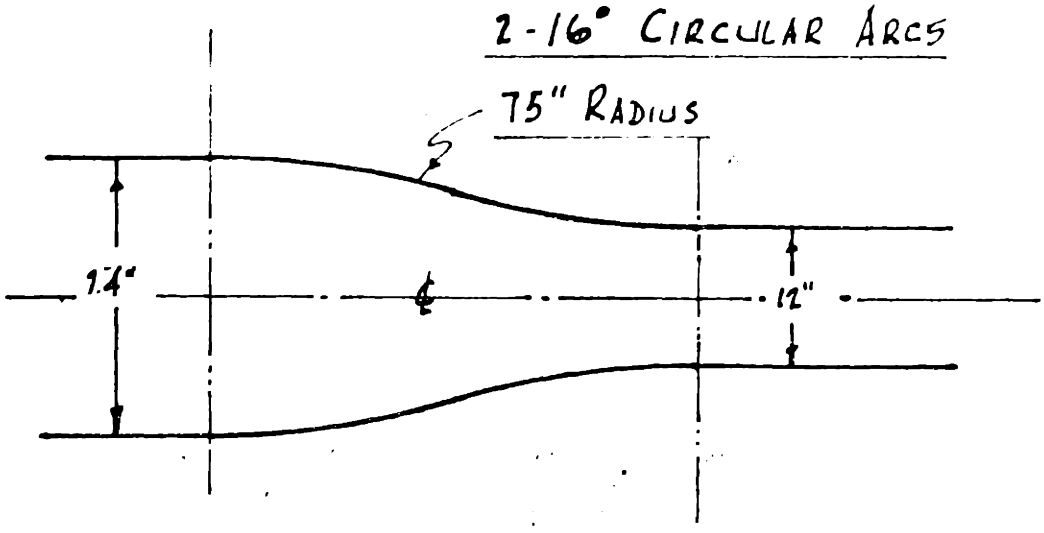

Figure 8

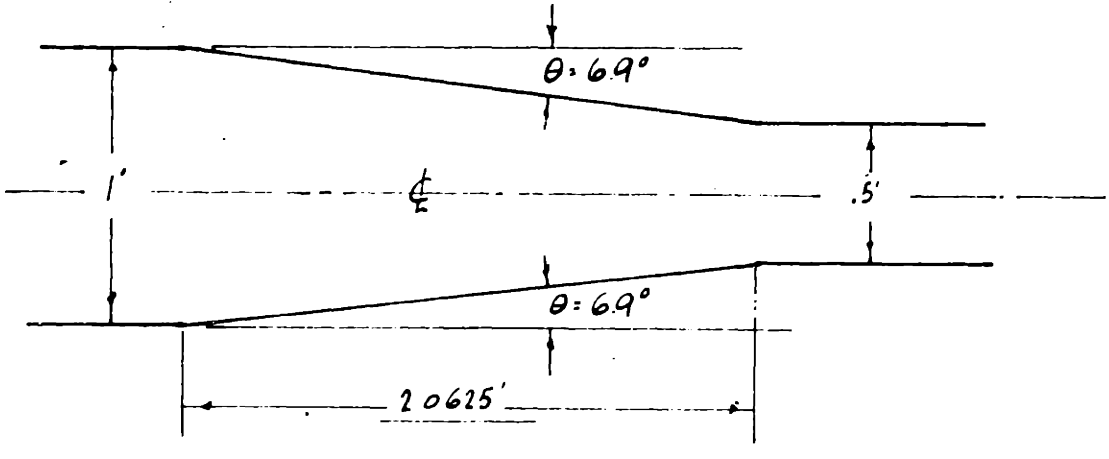

Figure 9

to Rodriguez's experiments at Froude numbers of 2.71 3.17, 3.56, and 4.00. The resulting characteristic diagrams, comparisons of experimental and theoretical side wall profiles, and the graphical constructions of the flow for these analyses are shown in figures 13-23 inclusive. Because of lack of experimental data, side wall profiles for F = 4 were not plotted.

NOTES ON THE USE OF THE METHOD OF CHARACTERISTICS

As pointed out previously, the characteristic curves are constructed from the differential equation of the flow. They are a plot in polar coordinates of $\overline{V}$ vs. θ. Their use enables on to analyze the flow in a channel and determine the effect that changes in diredtion have on the flow. The equation shows that the effect of a change in direction in supercritical flow is to change the velocity and the depth -- the characteristic curves make possible the quantitative determination of these changes.

To analyze a given flow, it is neceasary first to determine the $\overline{V}$ associated with the flow. $\overline{V}$ is a vector having magnitude and direction. It is usually most satisfactory to so orient the diagram that

the V_x axis of the diagram is parallel to the initial direction of flow in the channel. Since the Froude number of the flow is known, the magnitude of $\bar{V}$ may be directly determined from the relationship:

$$\bar{V} = \frac{F}{\sqrt{1+F^2}}$$

This equation is derived on page 53 in the appendix and plotted in figure 24.

The point of the vector $\bar{V}$ corresponds to a point on some epicycloid in the diagram. When the flow is deflected through an angle θ, the point of the velocity vector moves along the epicycloid and the vector is rotated to a new position in the diagram through the angle θ. The new point on the epicycloid represents a new region of the flow -- this region is characterised by the magnitude and direction of the velocity vector and the depth which is a unique function of $\bar{V}$ and is given by the relationship:

$$\frac{h}{H} = 1-\bar{V}^2$$

This equation is plotted in figure 25. The direction of the disturbance line or standing wave resulting from the change in direction of flow is given

by the mean of the perpendiculars to the epicycloid at the two points representing the regions of flow before and after the disturbance. This line is best drawn for small deflaction angles by taking the perpendicular midway along the epicycloid between the two points. The perpendicular is easily drawn using a graphical method which is very well described in Dr. Ippen's paper (7).

We now present without proof some general rules for the use of the method of characteristics. Full discussions of these points are to be found in Preiswerk's memorandum (5).

1. A point in the characteristic diagram describes the depth and the magnitude and direction of the velocity in a region of the flow plane.

2. When two disturbance lines of the same family (i.e. disturbance lines emanating from the s ame wall and thus represented by perpendiculars to the same family of epicycloids) meet, they converge to form one disturbance line. The three regions originally involved become two, the one between the two disturbance lines diaappearing and the upper and lower regions characterizing the new disturbance line.

3. When two disturbance lines of different families meet, they cross. The four regions involved form a parallelogram on the characteristics diagram. Since three of the regions are known before the lines cross, the fourth is always easily determined.

4. When a disturbance line meets a straight wall, it is reflected back into the flow. The three regions involved lie in a triangle on the characteristics diagram, the first and last regions lying on the same radial line. Since the first and second region are known, the third region is readily determined.

5. It is very valuable in making a study using this method, especially if the problem is complicated, to adopt some type of systematic numbering or lettering system for the points on the characteristic diagram. A careful study of figures 10 and 12 will show that this systematic approach gives a very good checking method in the flow plane. The author advocates no particular numbering system. But any systematic system yields valuable rewards in providing a continuous check against errors.

6. For flow along a smooth curved surface, such as the contraction in figure 8, the curve is broken

into 1, 2, or 4 degree arcs and approximated by a series of short straight lines. The accuracy of course increases as the increments are taken smaller.

DISCUSSION OF RESULTS

SYMMETRICAL CURVED CONTRACTION

Within the length of the contraction the theoretical and experimental side wall profiles are practically superimposed. although the experimental profile tends to lag the theoretical. This is probably due to viscosity which gives a lower velocity along the wall than the average. The lag is more considerable when the wave peak reaches the center of the contraction. In general the amplitude of the wave is decreased by viscous action in the contraction.

Beyond the contraction a diamond shaped wave is set up, both in theory and experiment. The tendency in the theoretical wave is toward a very high peak near the end of the contraction, this peak rapidly diminishing with ensuing waves. Theory shows that this diminution is due to the convergence of disturbance lines, and the resultant disappearance of those regions which are characterized by great depth. The theoretical curves show the same tendency. In a solely experimental study it would appear logical to assume that the diminution is due to viscous damping. It would be difficult, however, to explain the steep slope of the wave envelope in the early

part of the channel, and the gradual slope of the envelope in the lower regions. Here theory gives us the answer. The steep slope of the envelope, the rapid diminution of wave crests, is due primarily to dynamic damping, the convergence of disturbance lines to give disturbance lines of lesser intensity. In the lower regions of the channel, where all but two theoretical disturbance lines have converged and the remaining two are parallel and will never converge, the reason for the decrease in wave height is completely viscous damping. Here we get a true picture of the magnitude of the viscous effect.

In the region where the theoretical disturbance lines are parallel, the theoretical wave has a wave length of 2.7 feet. In the same region the actual wave has a wave length of 3.5 feet. The ratio of actual to theoretical wave length is 1.3. In this one test this value means little, but it would be interesting to determine from further research the factors which effect this ratio. If these factors are determinable, a step will have been made in the science of predicting wave action in advance of design.

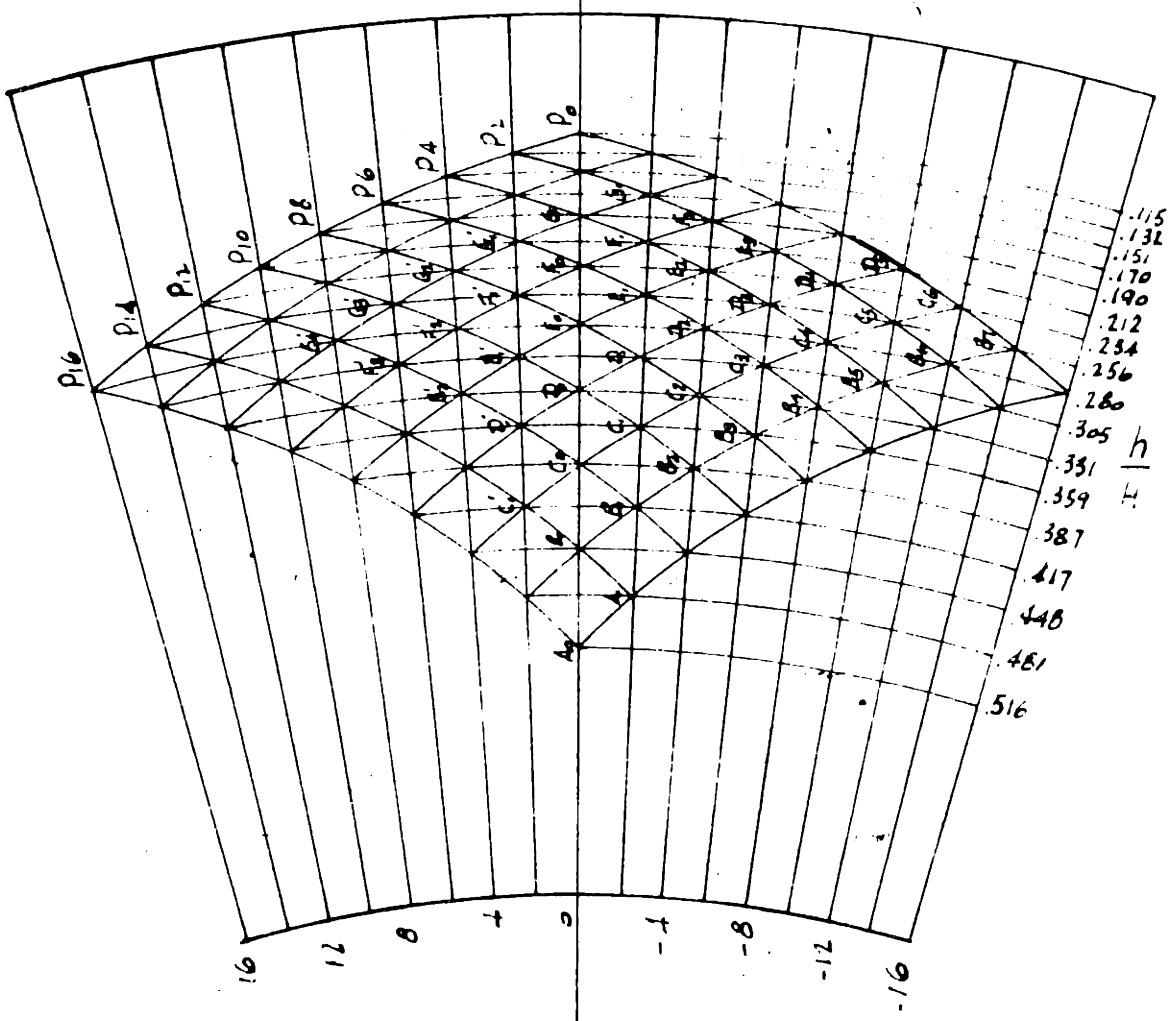

CHARACTERISTICS DIAGRAM

CURVED CONTRACTION

$\Gamma = 1$

FIGURE 10

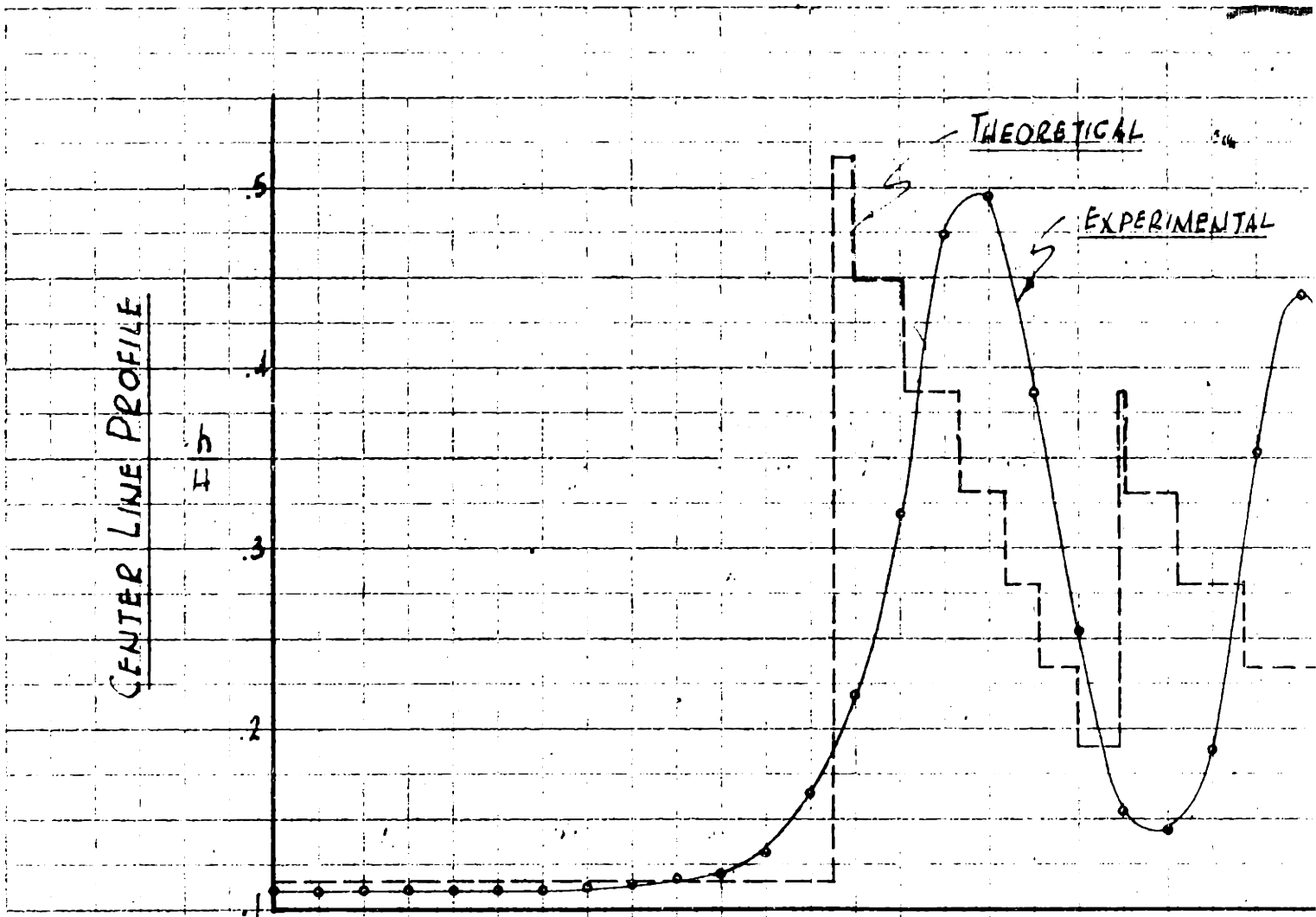

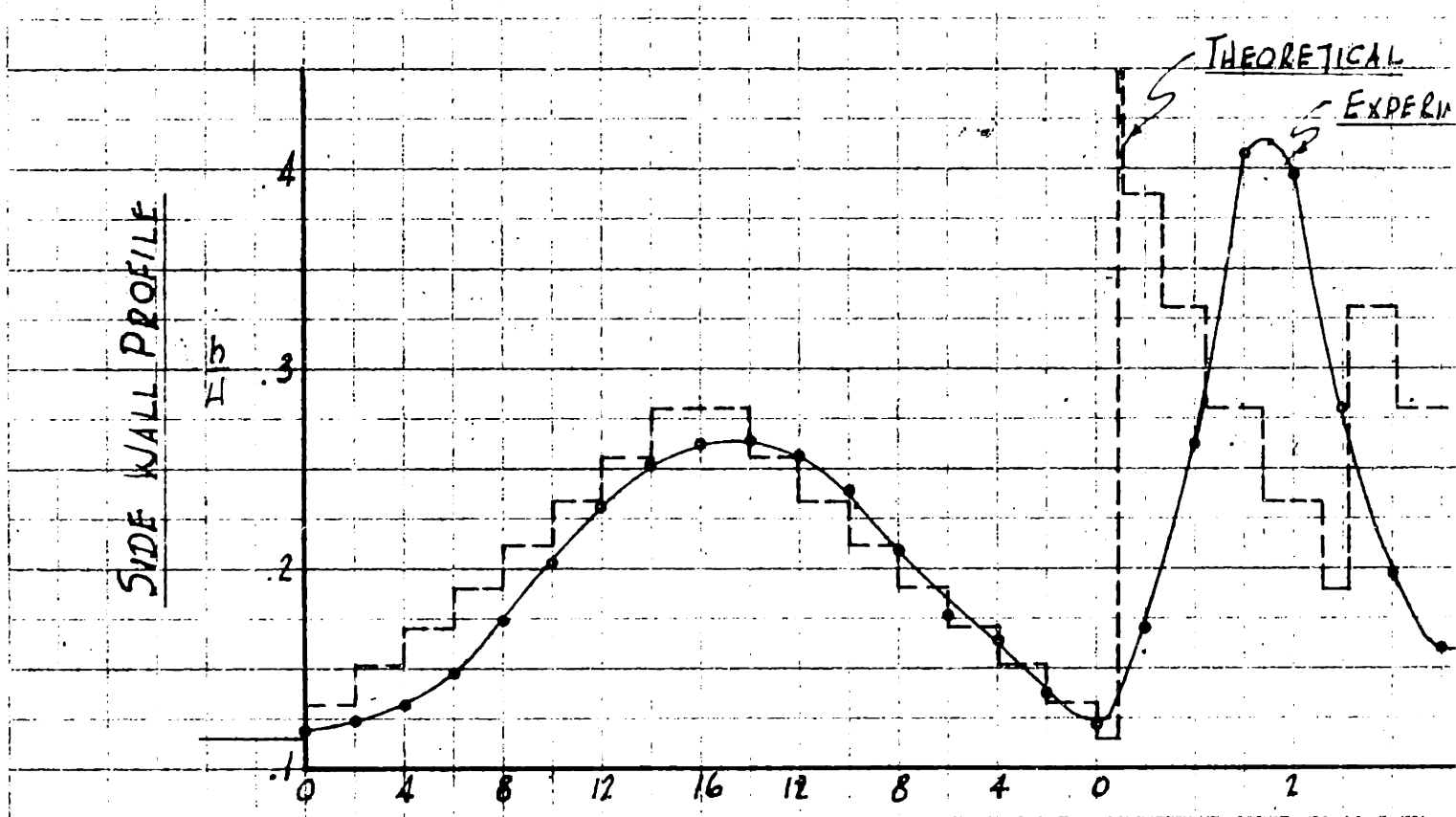

DISTANCE STATIONS ALONG C

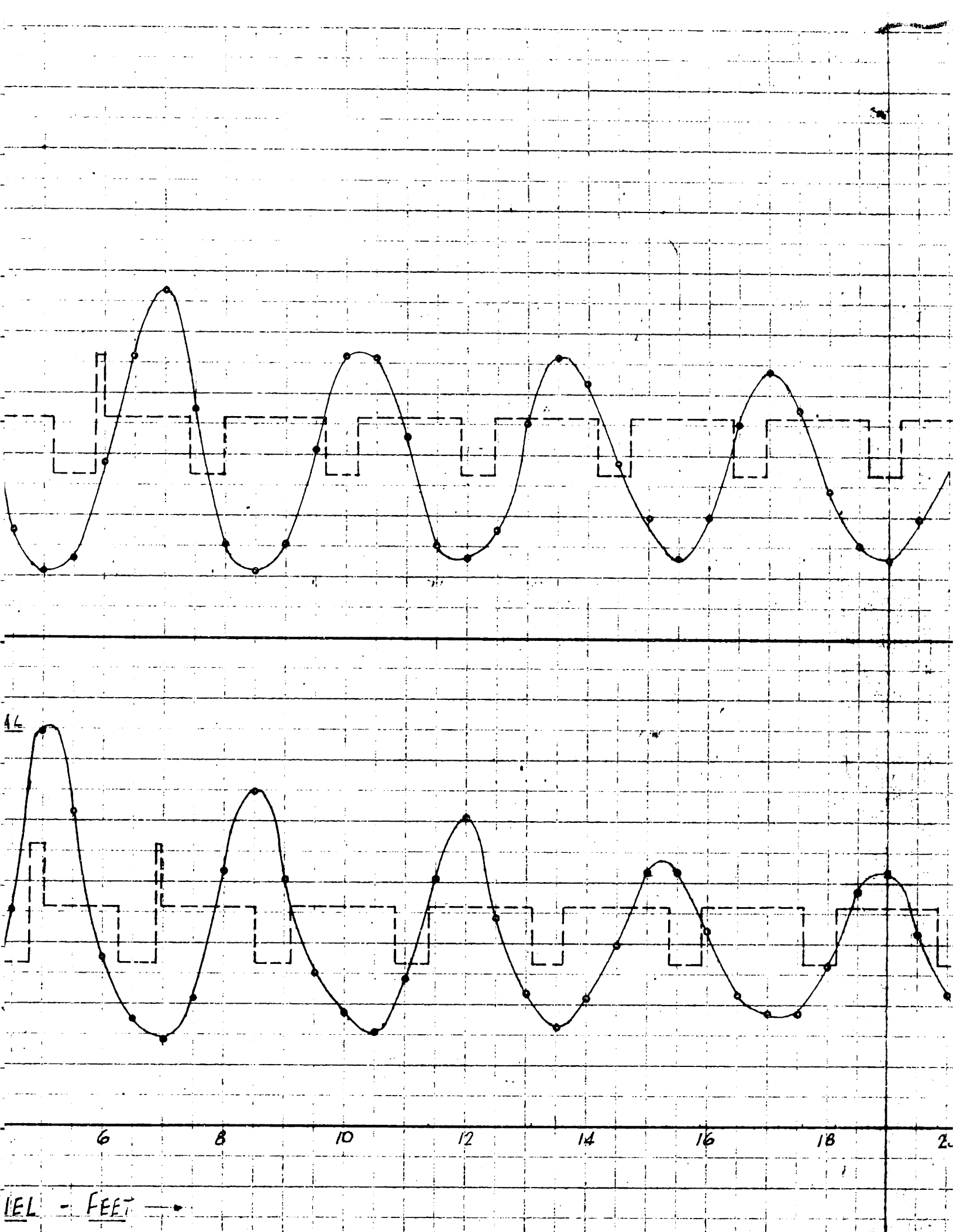
6
8
10
12
14
16
18
FEET

COMPARISON OF THEORETICAL & EXPERIMENTAL WATER SURFACE PROFILES

CURVED CONTRACTION

F = 4

FIGURE 11

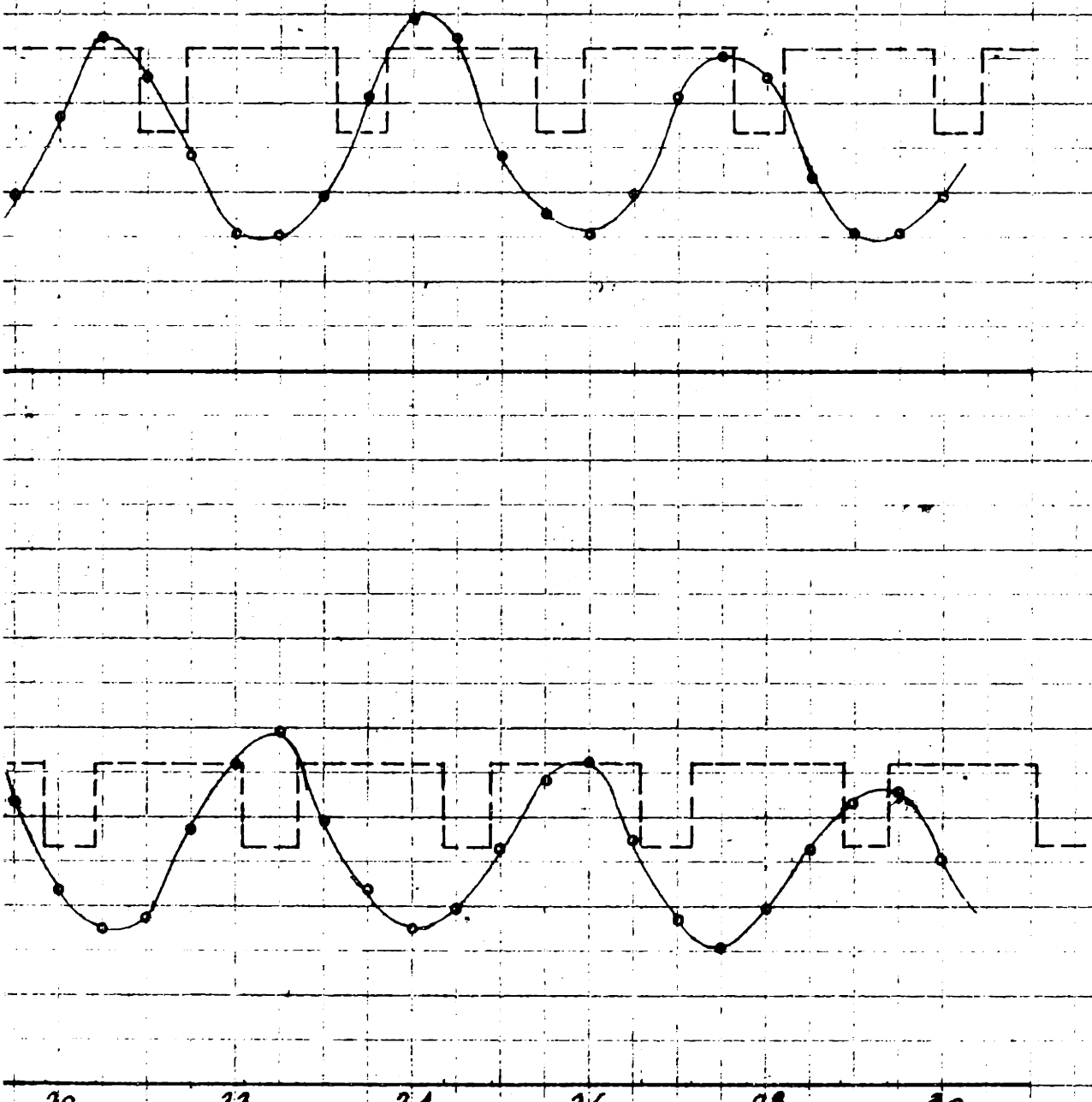

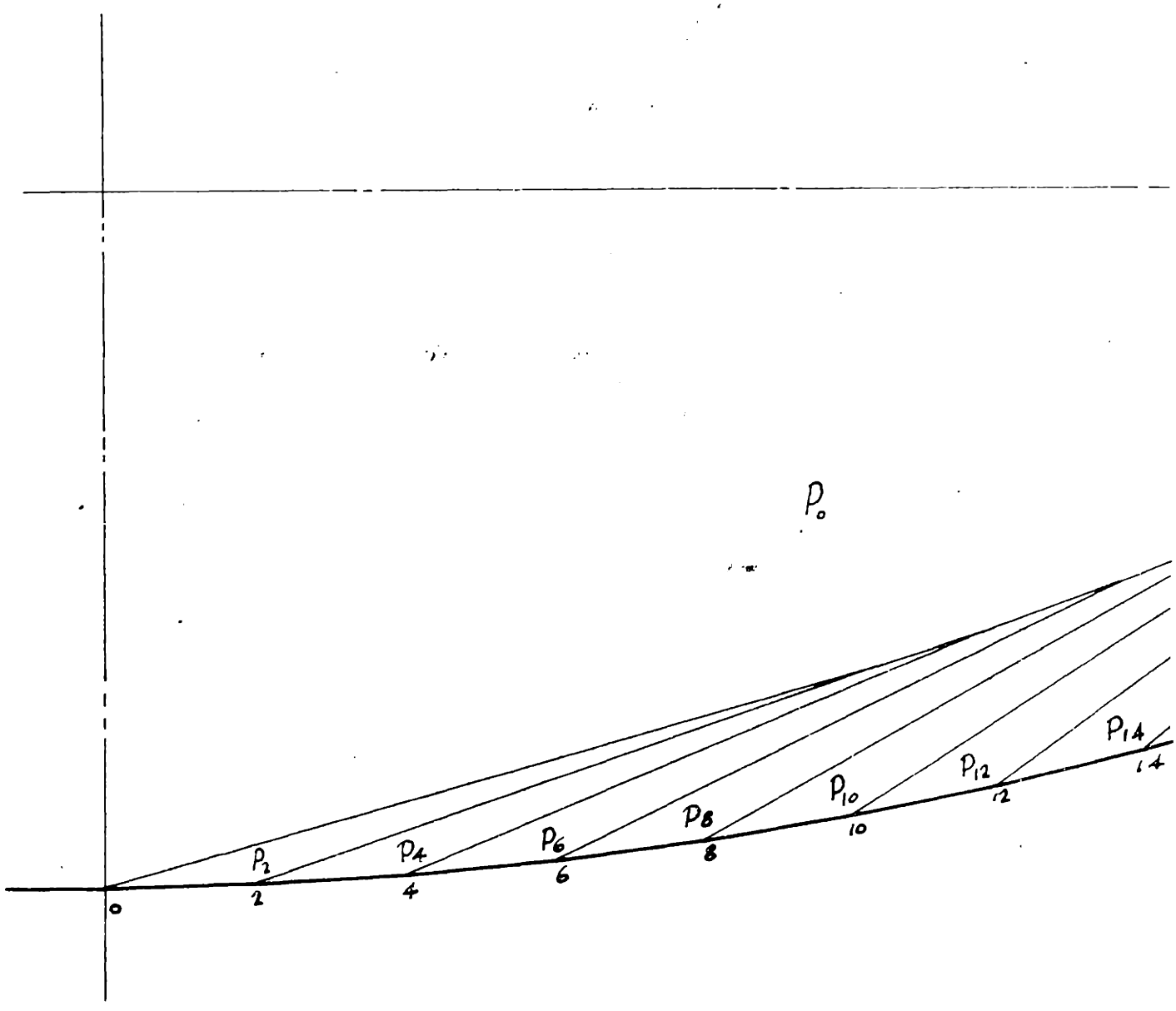
P_0
P_2
P_4
P_6
P_8
P_{10}
P_{12}
P_{14}
0
2
4
6
8
10
12
14

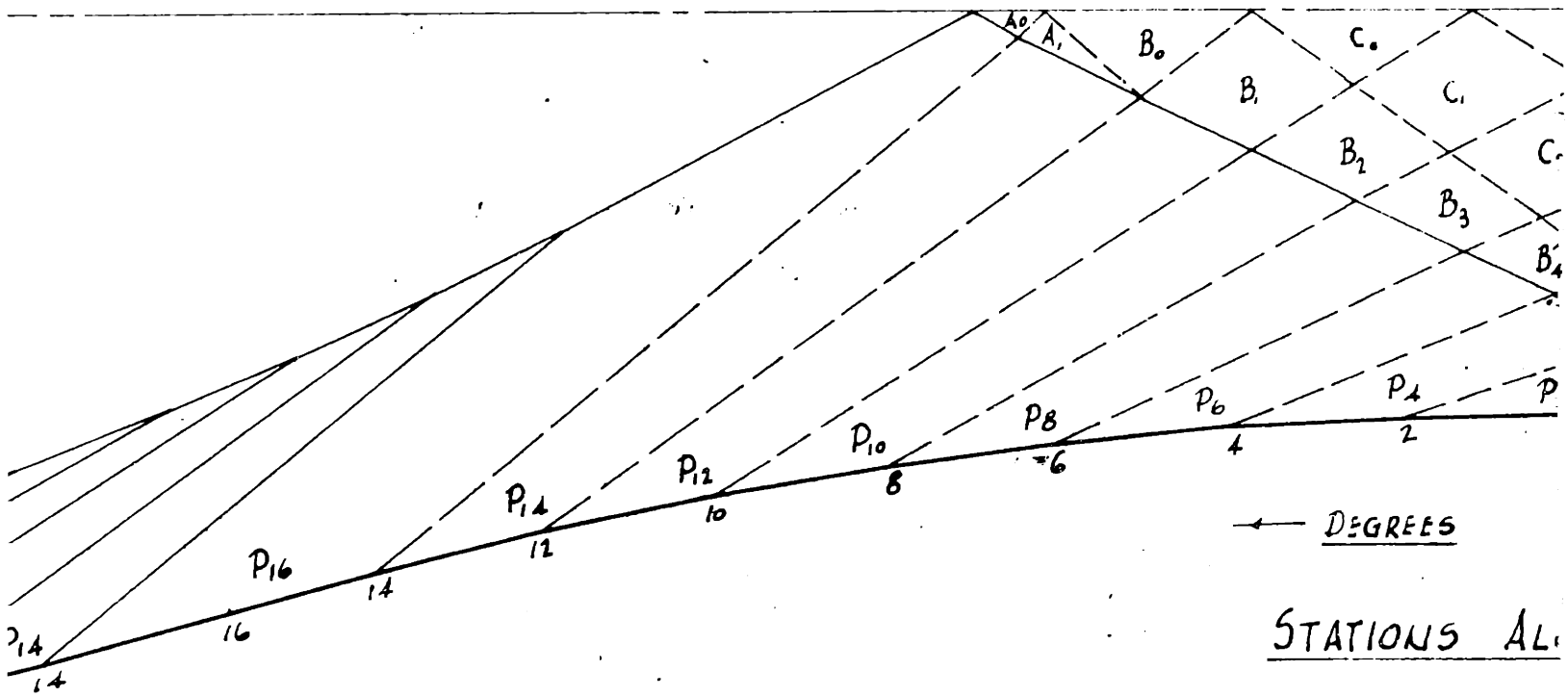
A0
A1
B0
B1
B2
B3
C0
C1
P16
P14
P12
P10
P8
P6
P4
16
14
12
10
8
6
4
2
DEGREES

STATIONS AL

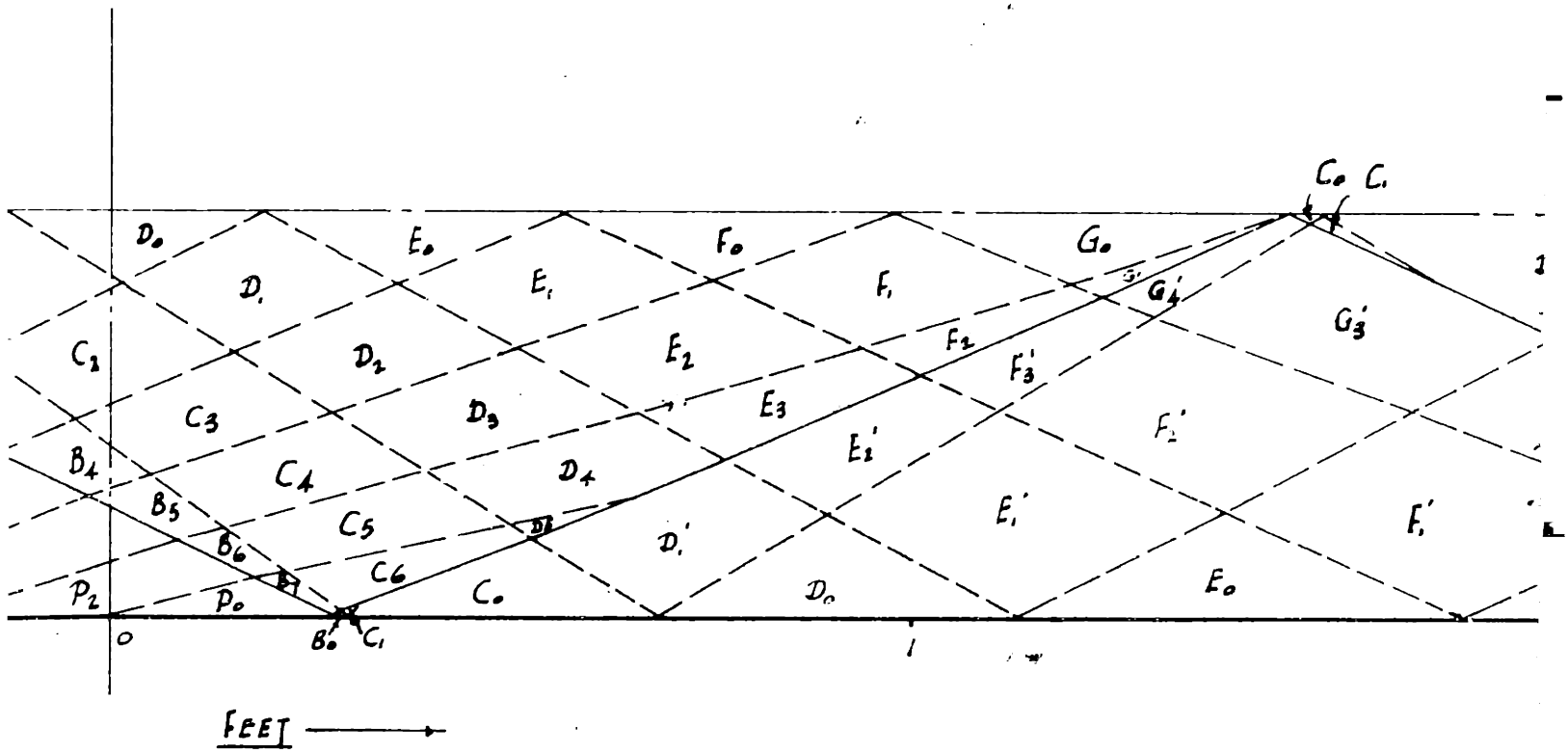

ALONG CHANNEL

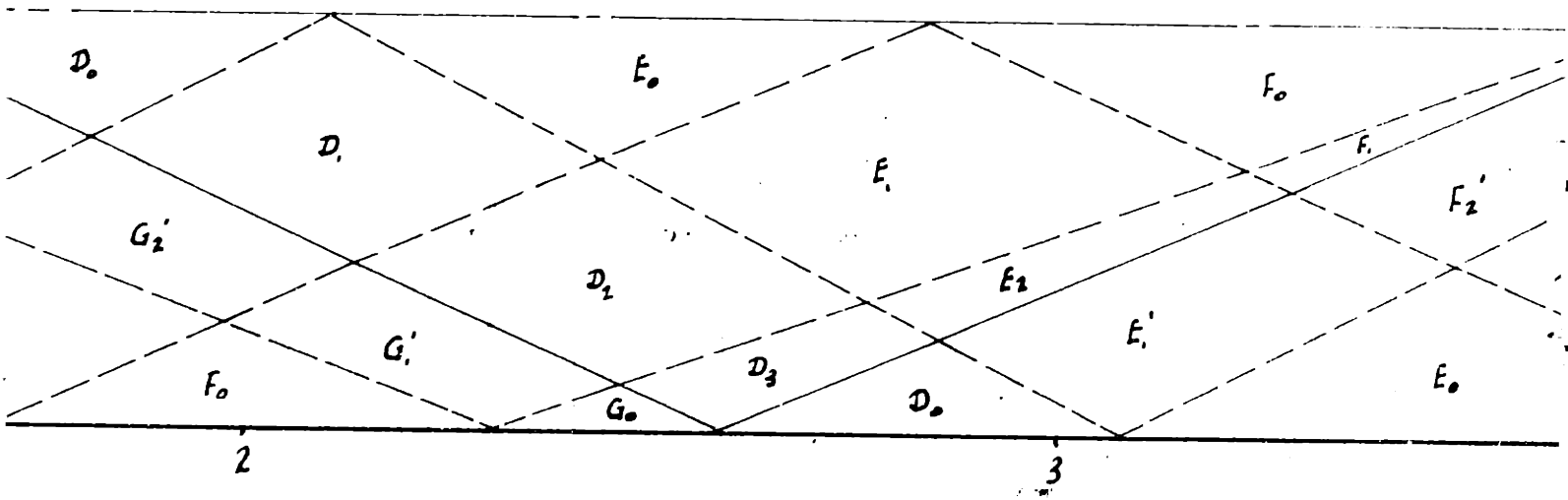
D_0
E_0
F_0
D_1
E_1
F_1
G_2'
F_2'
D_2
E_2
G_1'
E_1'
D_3
F_0
G_0
D_0
E_0
2
3

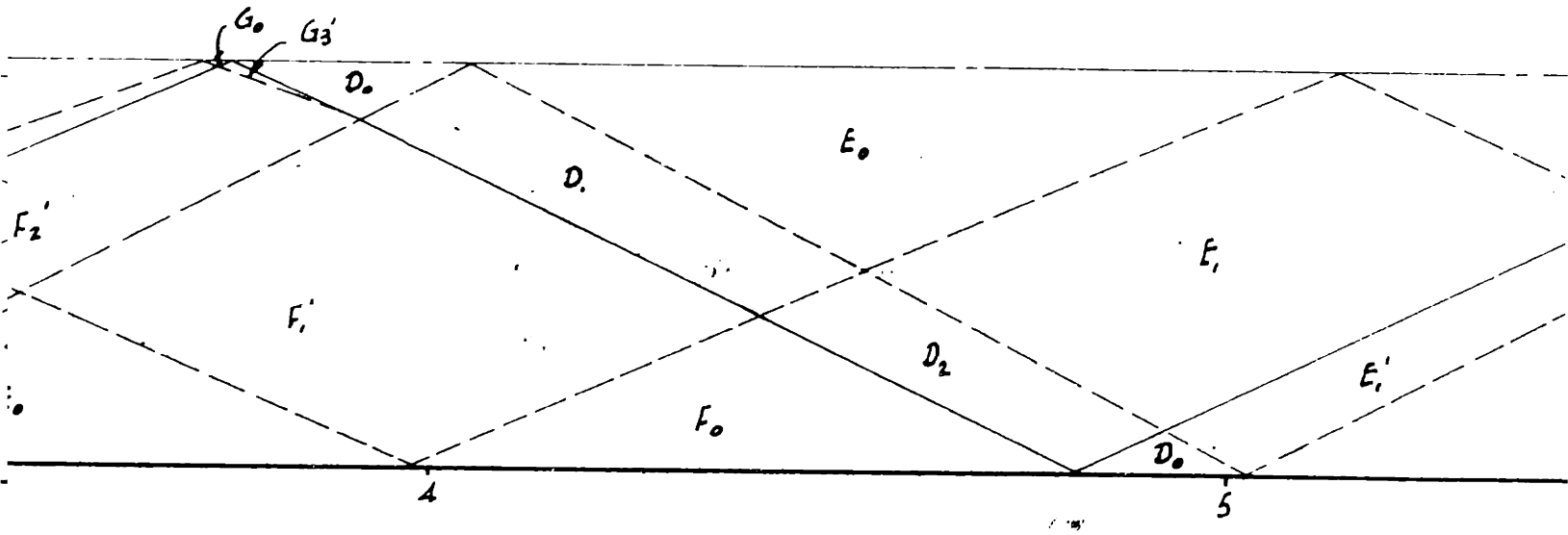
G₀
G₃'
D₀
E₀
D₁
F₂'
F₁'
F₁
D₂
E₁'
F₀
D₀
4
5

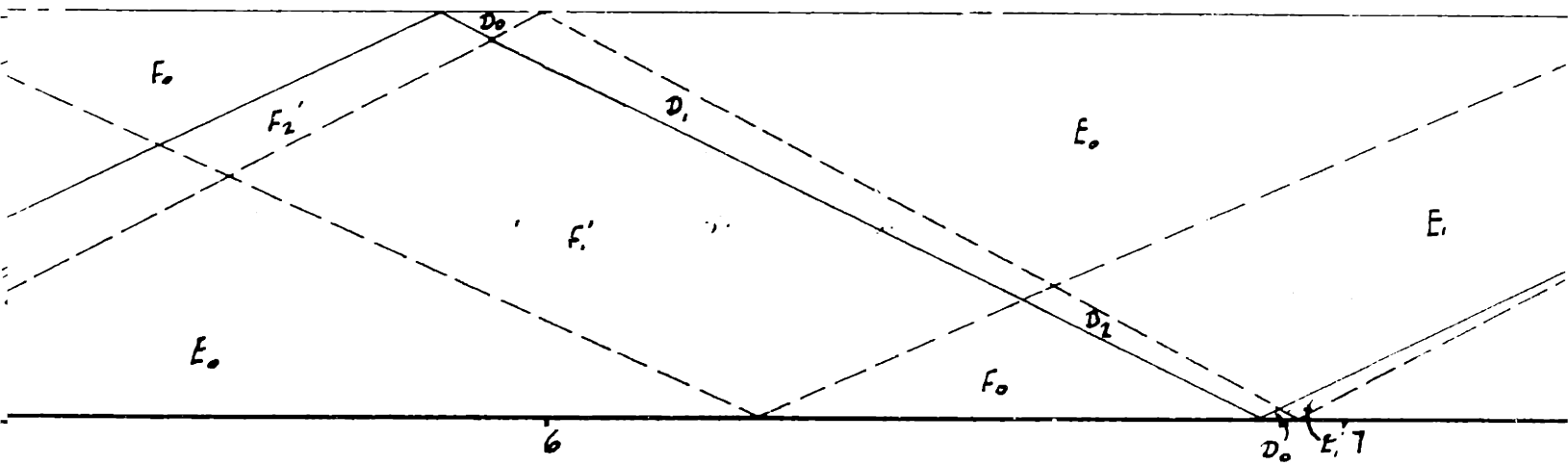
D_0
F_0
F_2'
D_1
E_0
F_1'
E_1
D_2
E_0
F_0
6
D_0'
E_1'
7

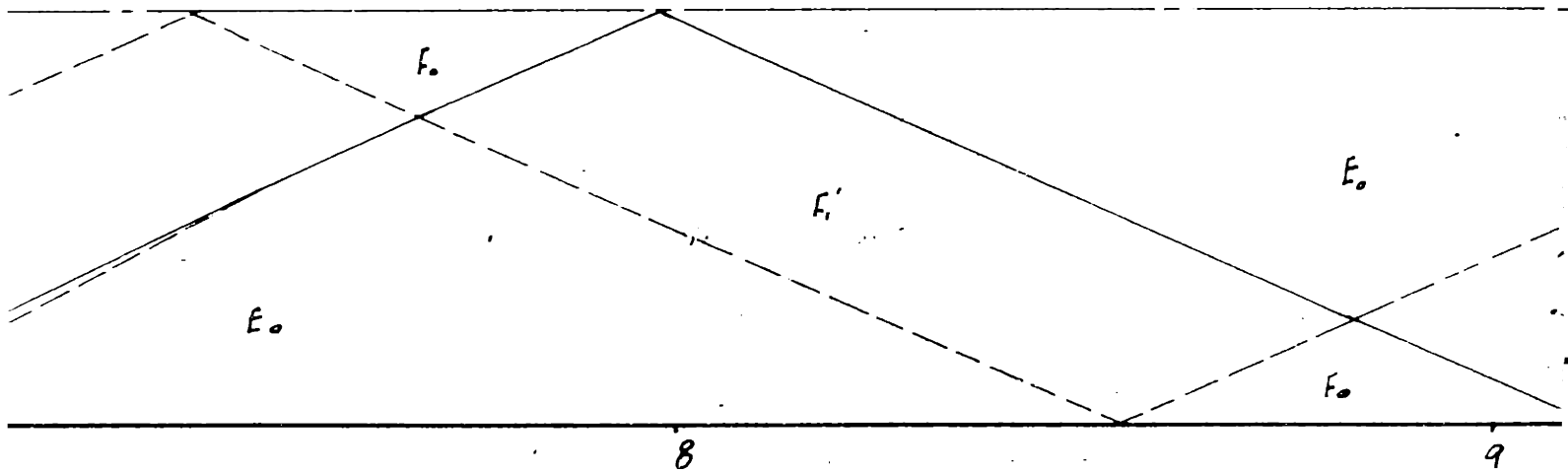
F₀
F₁'
E₀
E₀
F₀
8
9

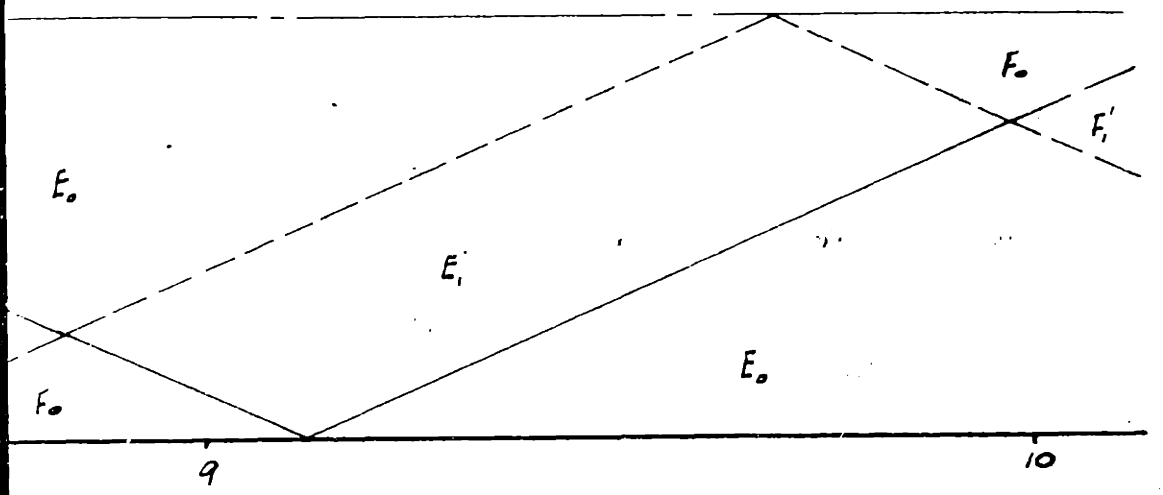

SYMMETRICAL CURVED CONTRACTION

FIELD OF FLOW

SHOWING DISTURANCE LINES

$F = 4$

FIGURE 12

6.9 SHARP ANGLE CONTRACTION

This channel was studied for values of F of 2.71, 3.17, 3.56, and 4.00. No experimental data were available for F = 4, but the channel was designed for this value. Accurately designed channels should be waveless at the design F. This channel appears to be slightly inaccurate, as shown by the disturbance lines in the field of flow. If the channel were correctly designed, the disturbance line originating at the upstream angle of the contraction would be reflected in such a manner that it just met the downstream angle of the contraction. Here an equal and opposite disturbance line is propagated, which would exactly cancel the first disturbance, leaving the channel waveless. As the channel is designed viscosity would undoubtedly brigg about a quick damping of the wave which develops.

At F = 2.71 the side wall profile plot shows quite good correlation within the contraction. The increases in depth are of course sudden in theory, whereas again in practise viscosity smooths out all sudden changes and smooth curves result. The disturbance wave propagated at the beginning of the contraction results in a sharp rise both in theory and

experiment. This wave when reflected back to the wall gives another sharp rise theoretically, but actually its influence has spread out and it is evidenced only by an inflection of the curve upward.

Theoretically - see the characteristics diagram, figure 13 - the flow jumps into the subcritical range toward the end of the contraction. In reality it does not do this, but remains in the supercritical range. Apparently the slope of the channel is sufficient to maintain supercritical flow, whereas the theory assumes a level channel.

Here a problem arises. The characteristic diagram gives no information for subcritical flow. We are faced with the problem of plotting the depth in the subcritical portion of the channel. A relationship is derived on page 56 of the appendix, stating:

$$\left(\frac{h}{H}\right)^2 - \left(\frac{h}{H}\right)^3 = \frac{Q^2}{2gHb^2} = \frac{A}{b^2}$$

We may determine A at any point in the channel, since it is a constant throughout the channel. If we choose the entrance, where h/H = 0.213 and b = 1 ft.:

$$A = b^2\left[\left(\frac{h}{H}\right)^2 - \left(\frac{h}{H}\right)^3\right]$$

$$= 1\left[.0454 - .0097\right] = .0357$$

At the contracted section b = 0.5'

$$\left(\frac{h}{H}\right)^2 - \left(\frac{h}{H}\right)^3 = \frac{.0357}{(0.5)^2} = .1428$$

This gives h/H = 0.737, which we sought.

At F = 3.17 quite good correlation was obtained in the contraction, as at F = 2.71. On leaving the contraction theoretical and actual flows both show a drop and subsequently a rise. The several individual waves of the theoretical solution are replaced by a much longer wave in the experimental flume. At F = 3.56 this same phenomenon is noted. This seems to show a lack of accuracy in the theory. Further study may show some correlation between these two wave types.

CONCLUSIONS

The method of characteristics has been shown to show the trend of wave patterns in channels with flow at supercritical velocities. An experienced man, faced with the design of a channel contraction, can make a theoretical study of a proposed contraction and predict quite accurately the wave forms which will be present in the contraction at various Froude numbers and draw the sidewall and centerline profiles which would result.

Beyond the contraction the effects are not so well defined. In the curved contraction it seems that some correlation could be found between theoretical and actual wave length. Amplitudes of the waves are predictable with some degree of accuracy. In the sharp angle contraction wave forms beyond the contraction were very poorly approximated by theory.

It has been indicated, but not conclusively shown, that the method is most accurate between Froude numbers of 3.5 and 7.0, that below this range the effect of viscosity is considerable, and that at higher Froude numbers the assumption of hydrostatic pressure distribution loses its validity.

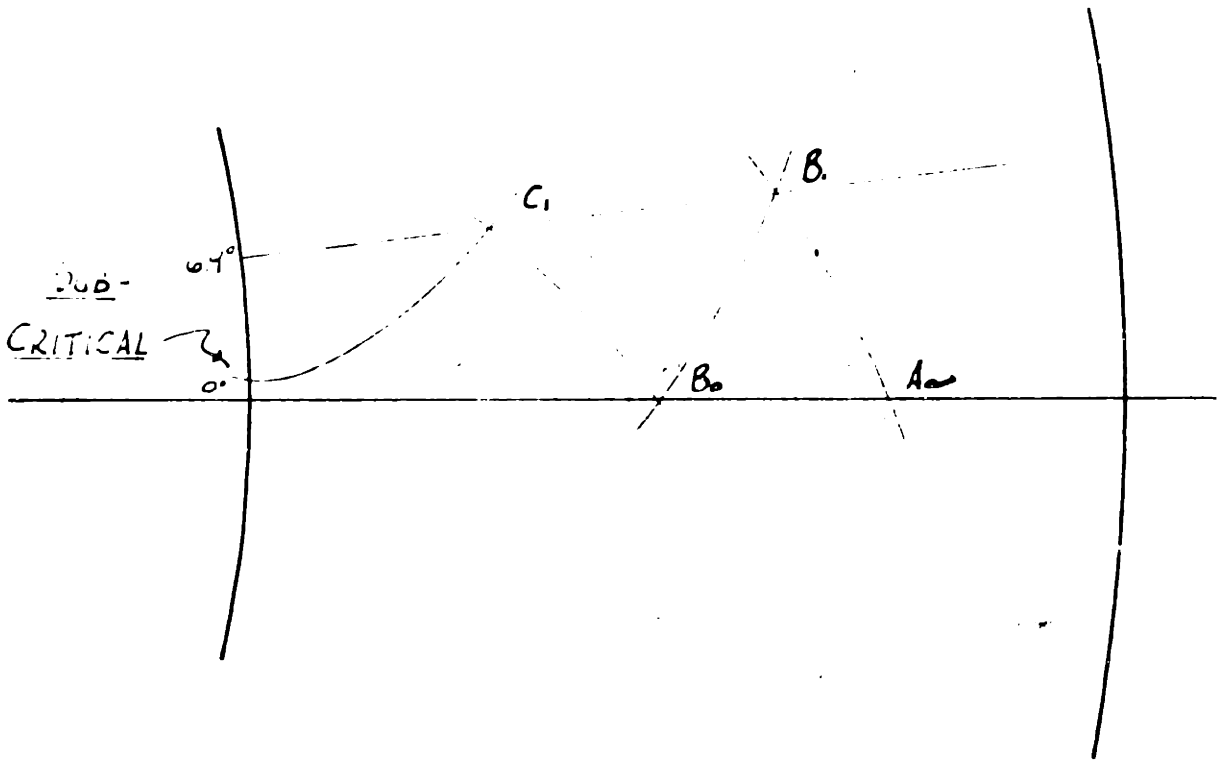

CHARACTERISTICS DIAGRAM

6.9° CONTRACTION

$\mathbb{F} = 2.71$

FIGURE 13

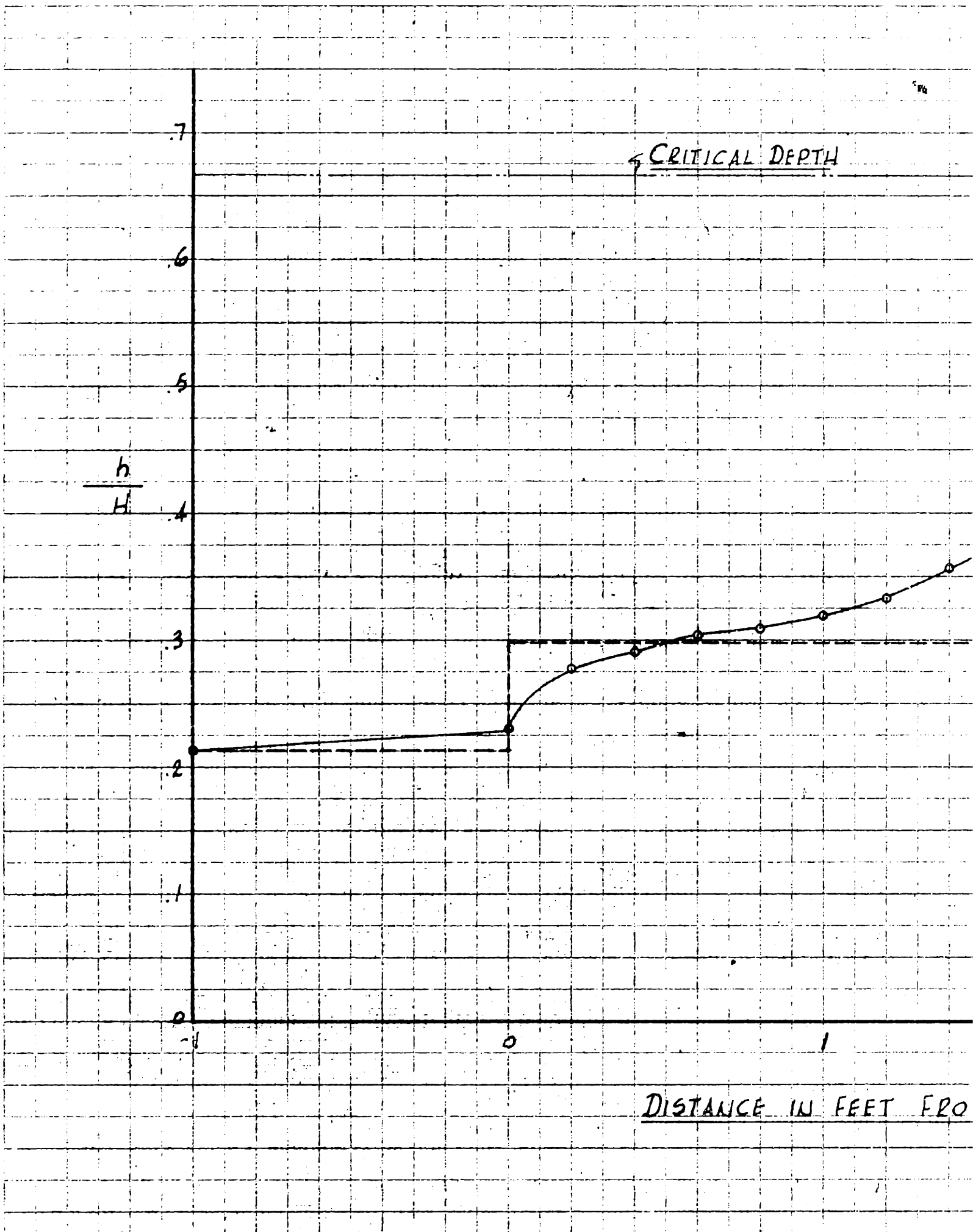
CRITICAL DEPTH
h/H
.7
.6
.5
.4
.3
.2
.1
0
-1
0
1
DISTANCE IN FEET FRO

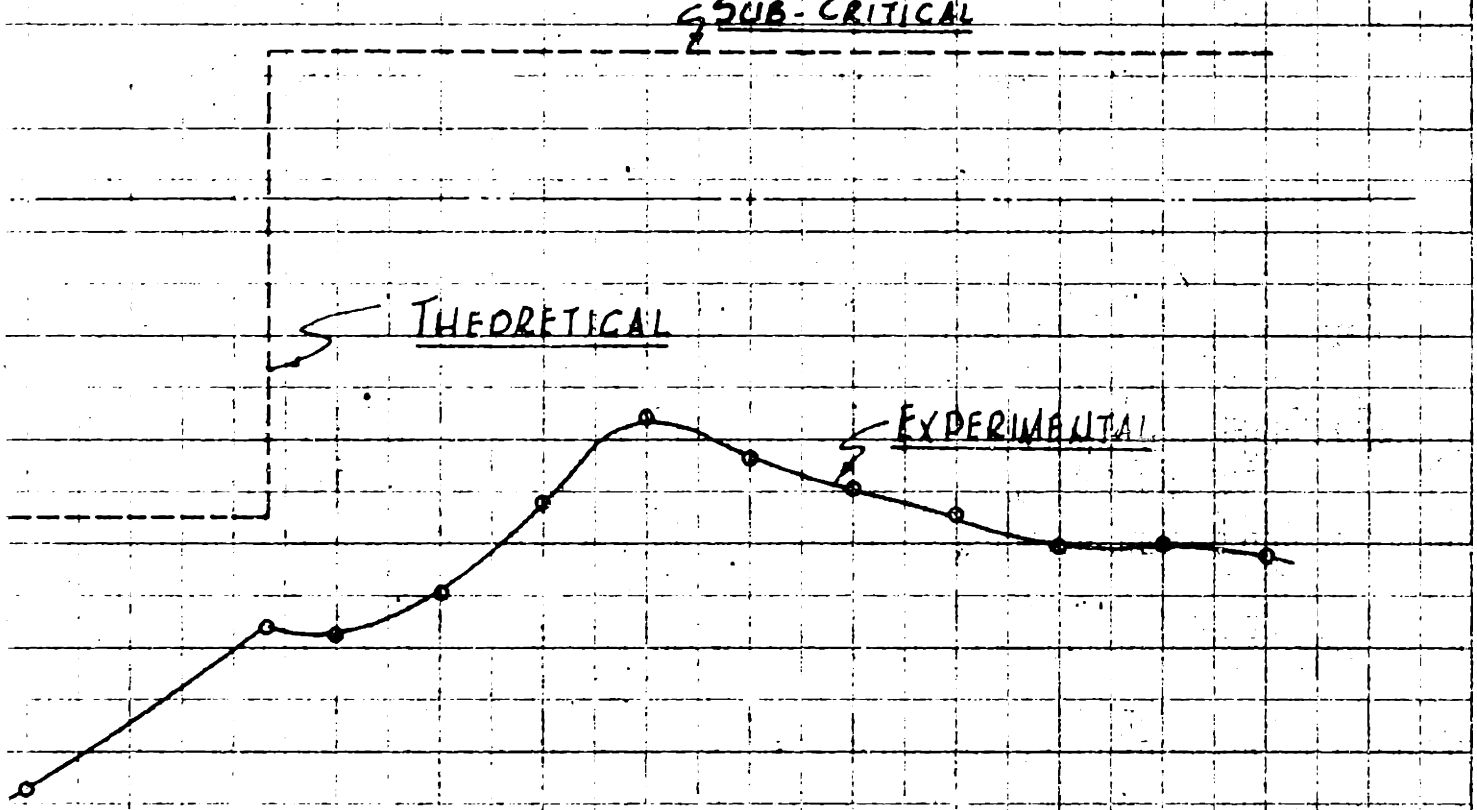

COMPARISON OF THEORETICAL & EXPERIMENTAL SIDE WALL PROFILES

6.9° CONTRACTION

$\bar{F} = 2.71$

FIGURE 14

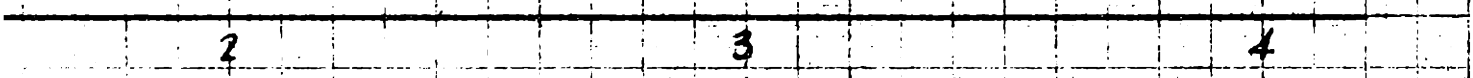

CONTRACTION ENTRANCE

STATIONS ALONG

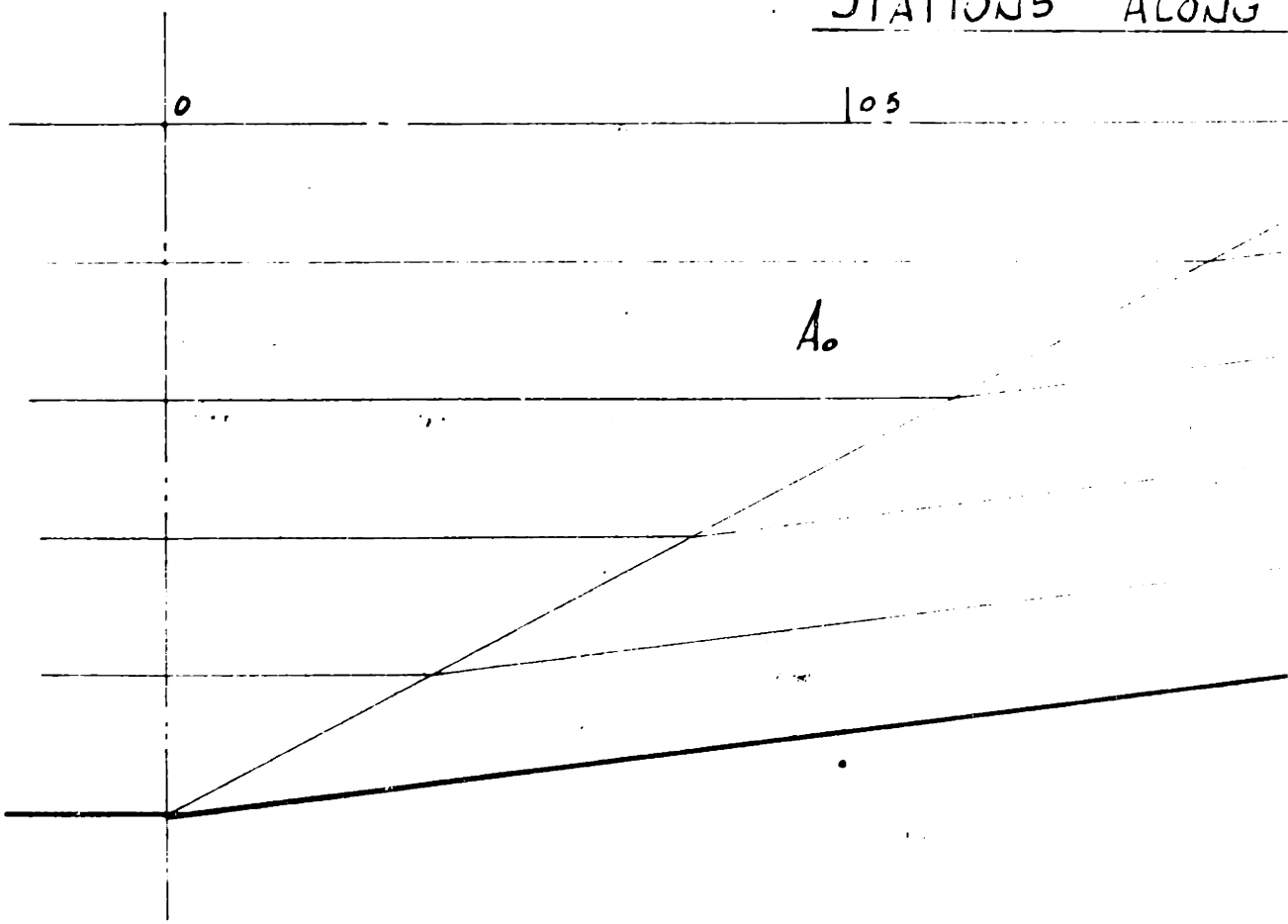

ALONG CHANNEL - FEET

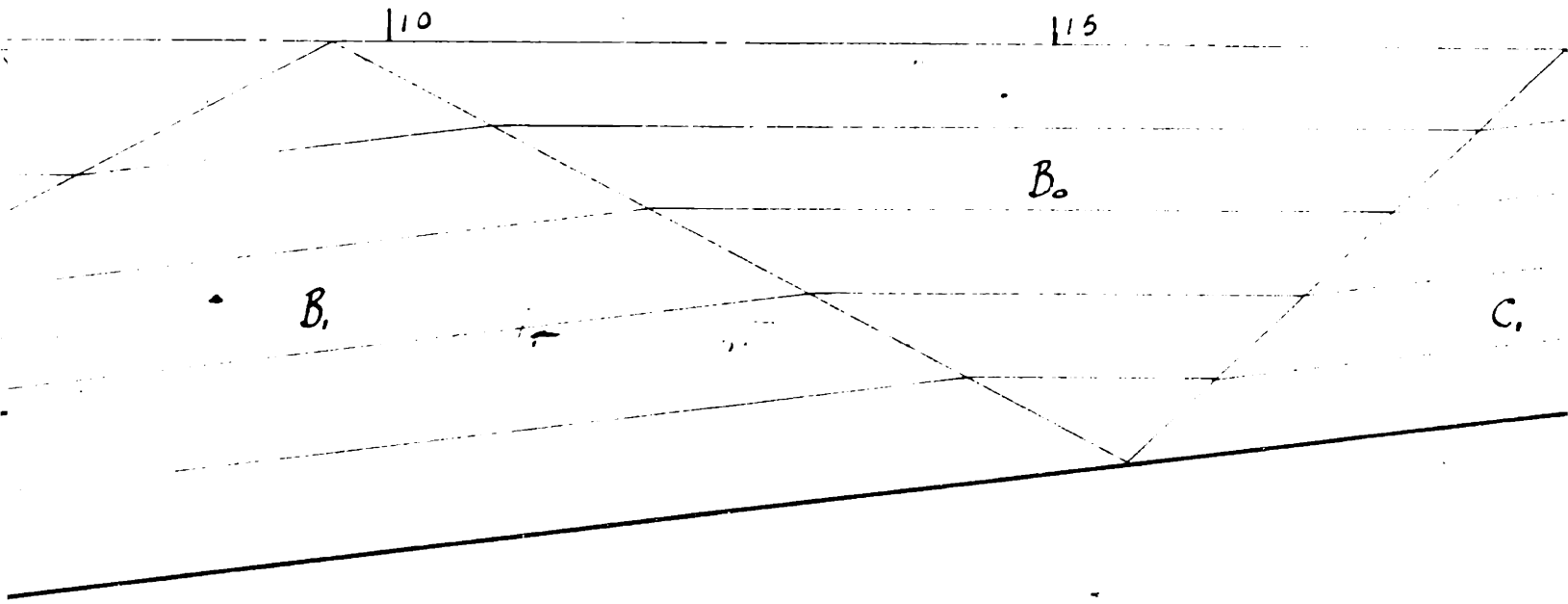

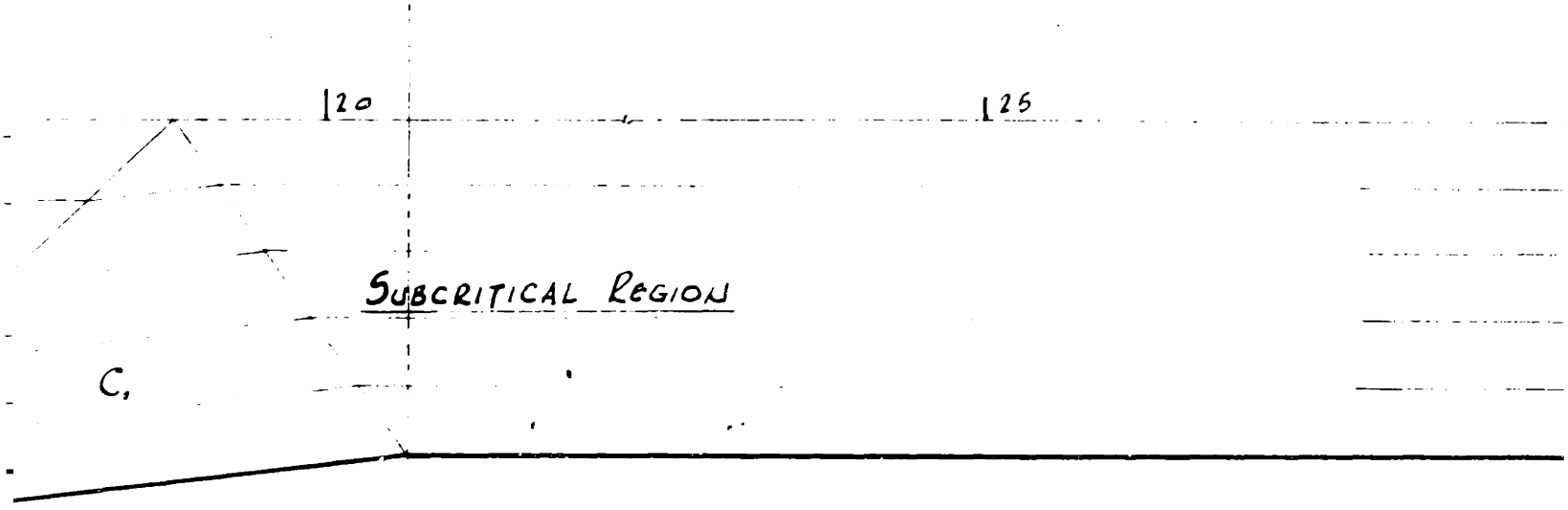
120
125
SUBCRITICAL REGION
C,

30

35

6.4° SYMME
SHARP ANGLE

FIELD OF F
SHOWING STREAM & DIST
F = 2.7
FIGURE

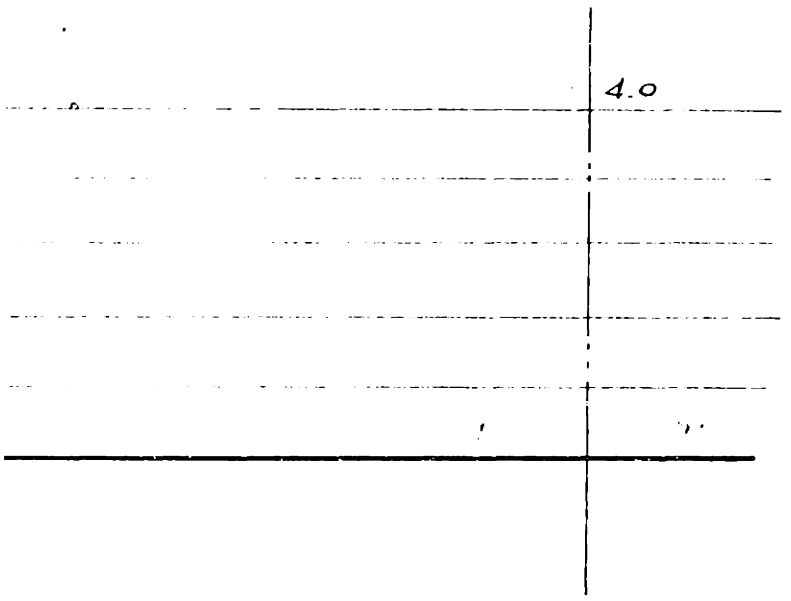

6.4° SYMMETRICAL
SHARP ANGLE CONTRACTION
FIELD OF FLOW
SHOWING STREAM & DISTURBANCE LINES
$\mathbb{F} = 2.71$
FIGURE 15

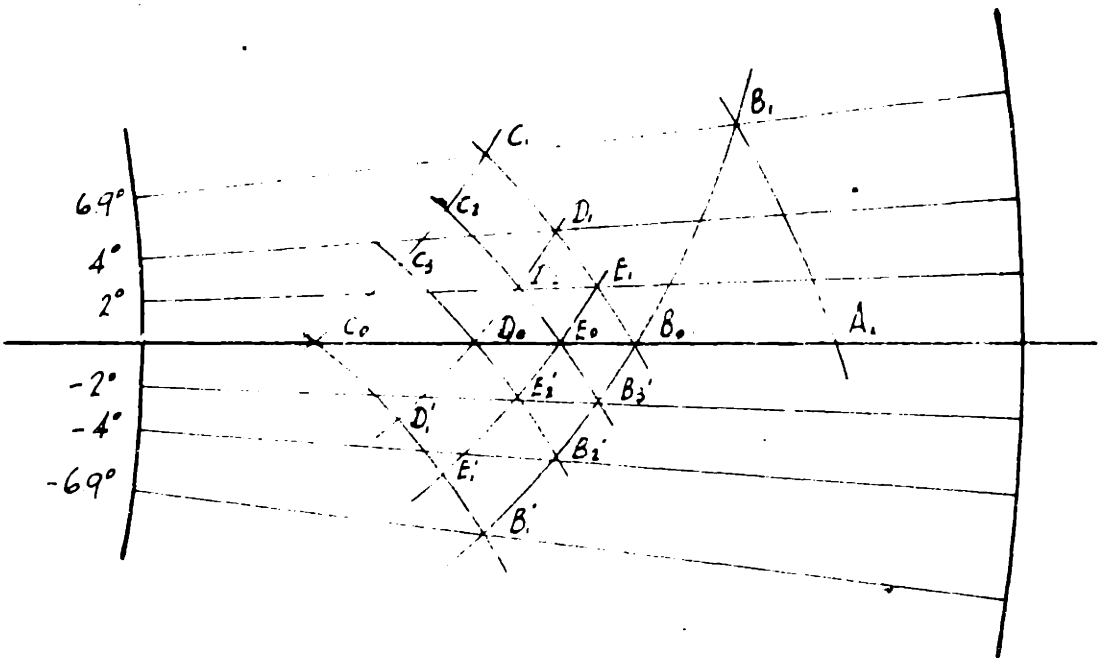

CHARACTERISTICS DIAGRAM
6.9° CONTRACTION
F = 3.17

FIGURE 16

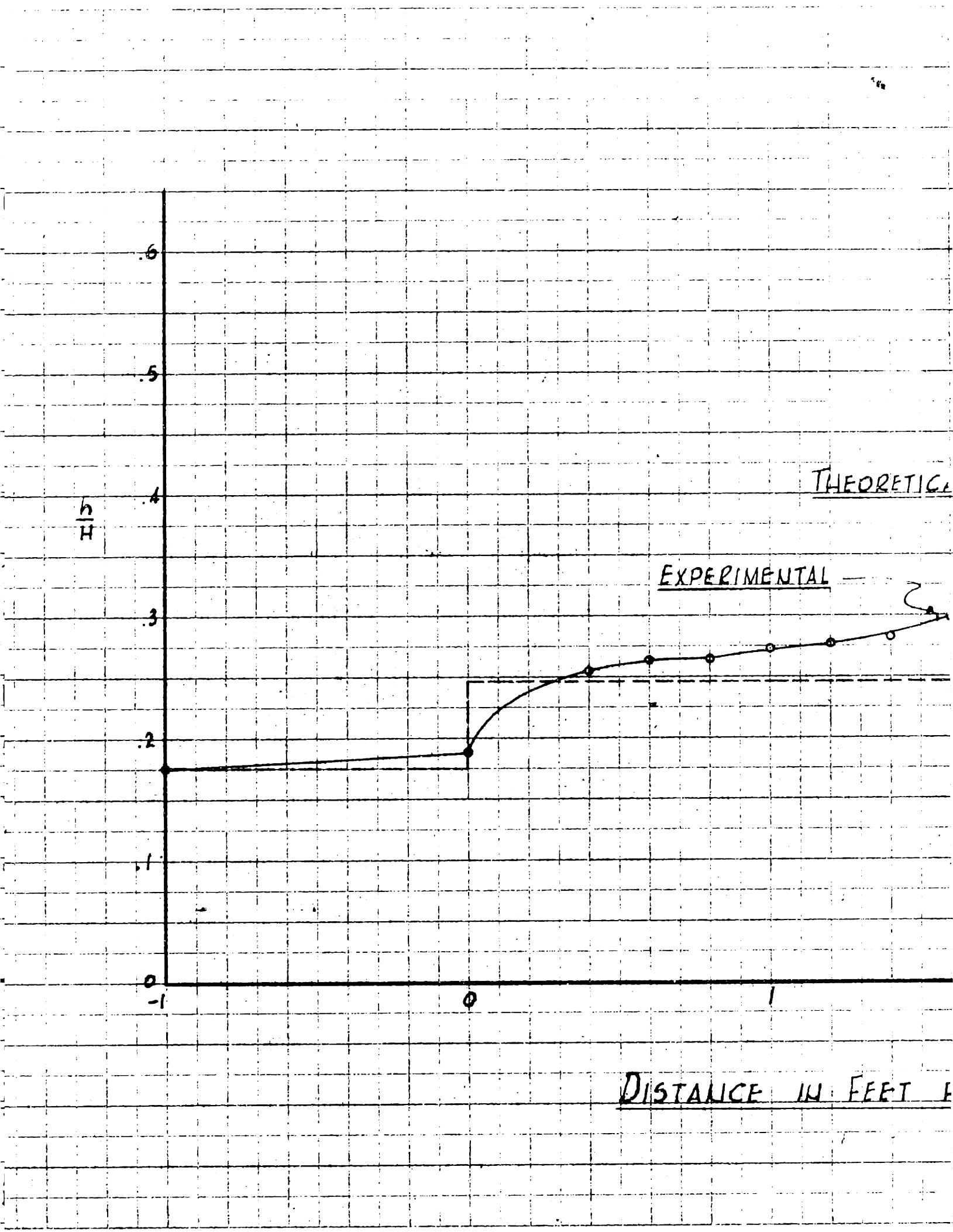
.6
.5
h/H
.4
.3
.2
.1
0
-1
0
1
THEORETICA
EXPERIMENTAL
DISTANCE IN FEET F

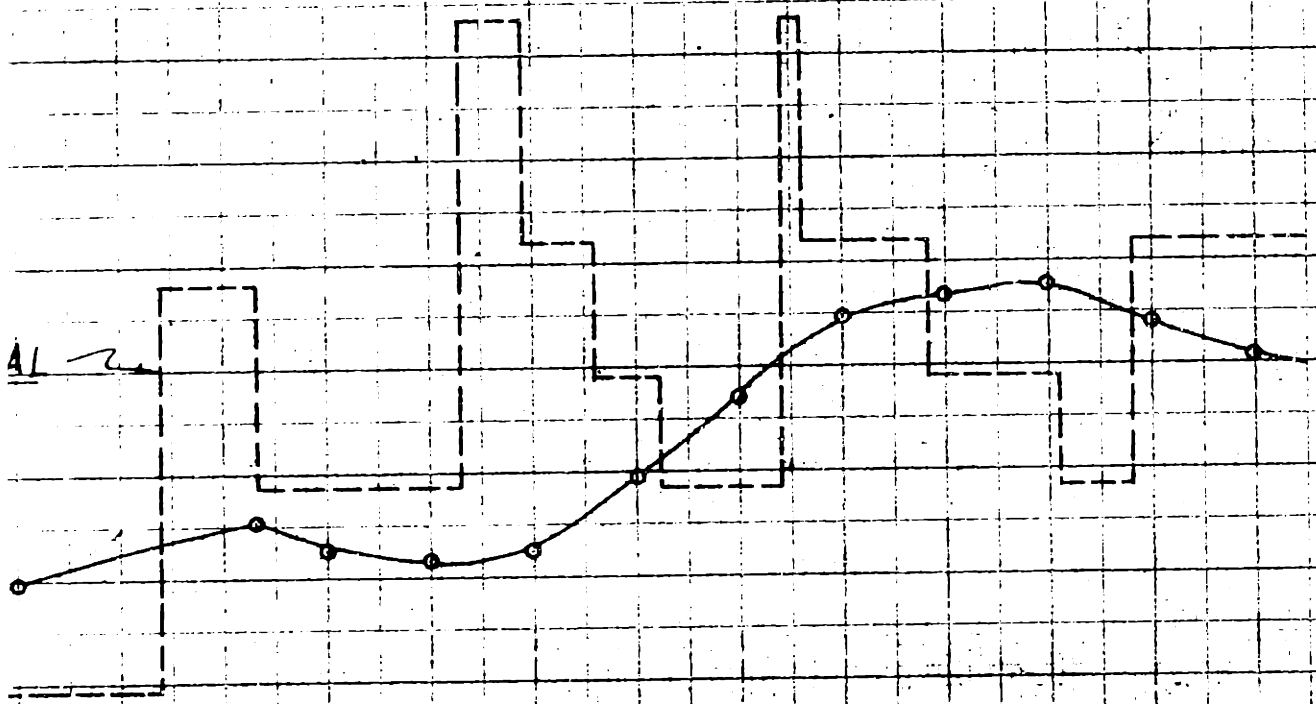

COMPARISON OF THEORETICAL & EXPERIMENTAL SIDE WALL PROFILES

6.9° CONTRACTION

$\mathbb{F} = 3.17$

FIGURE 17

STATIONS A

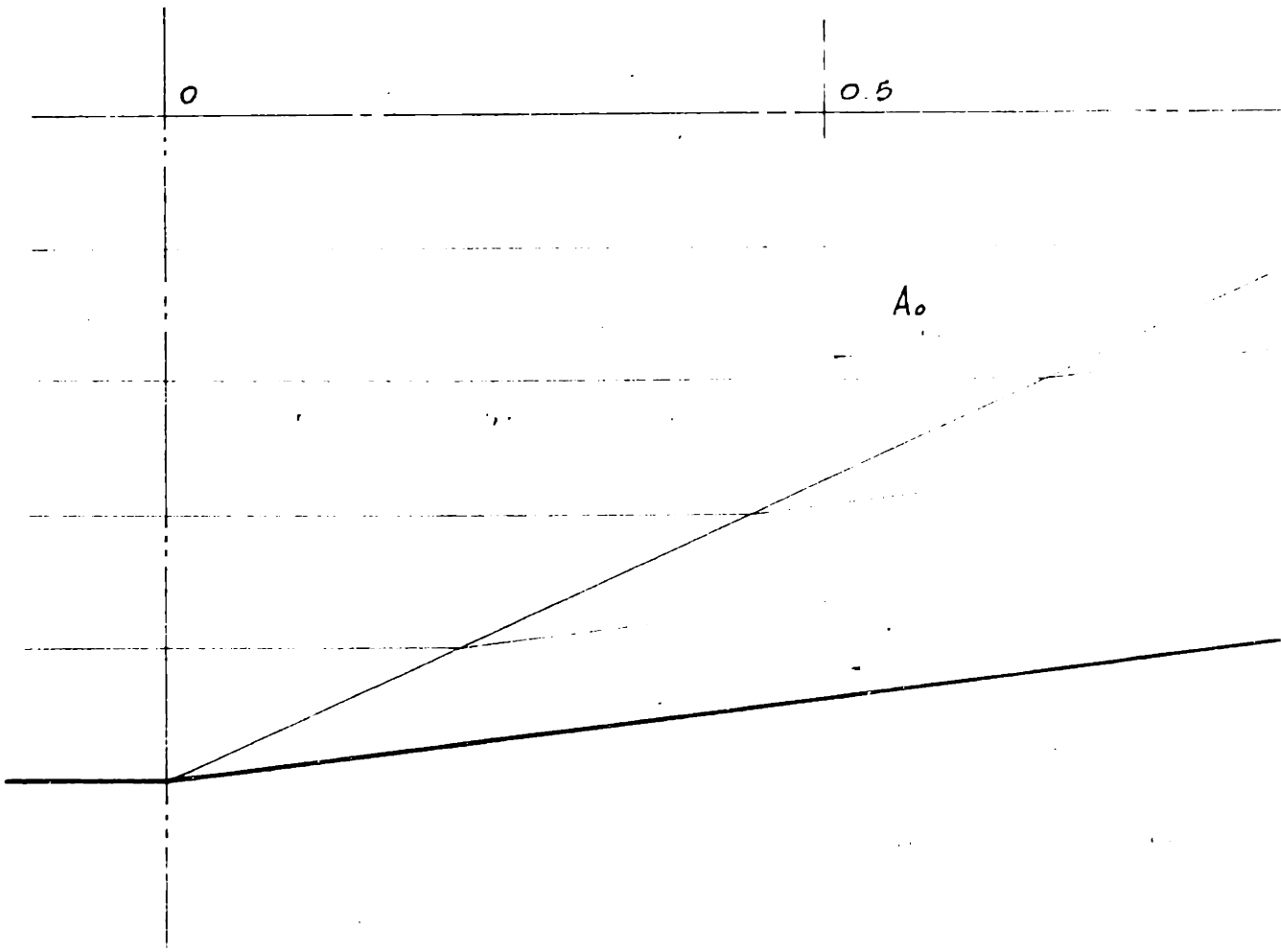

IONS ALONG CHANNEL - FEET

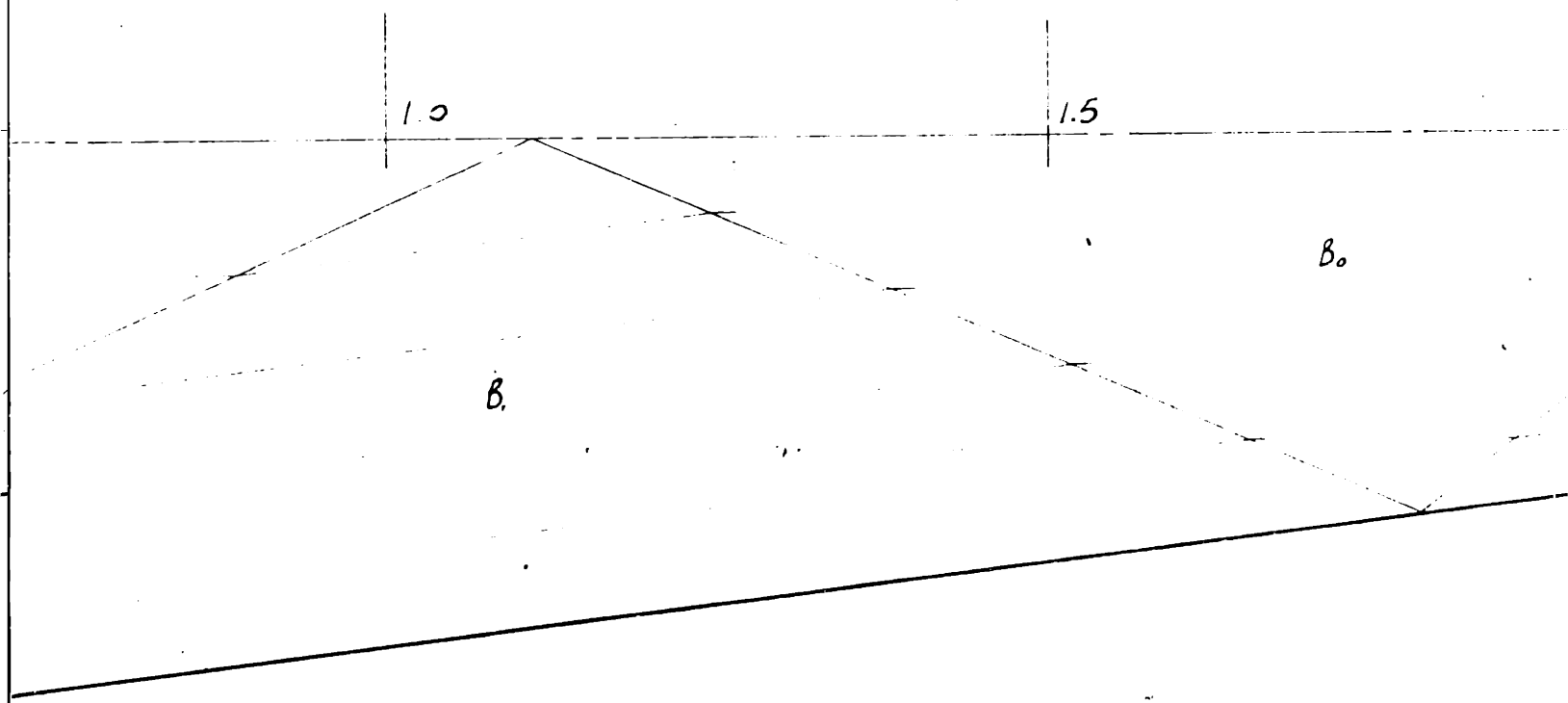

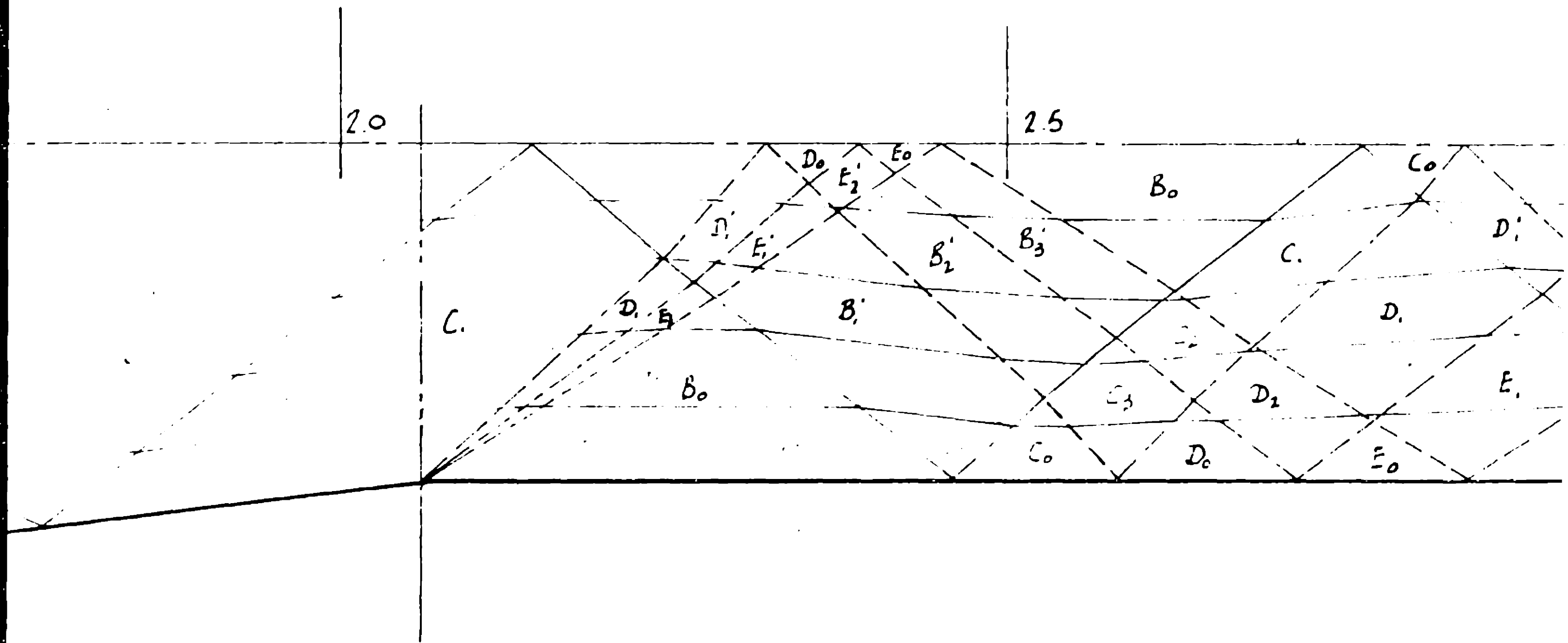

2.0
2.5
C.
D. E
B.'
B₀
D'
E'
D₀
E₂'
E₀
B₂'
B₃'
B₀
C.
C₀
D.'
D.
E.
C₀
D₀
E₀
D₂

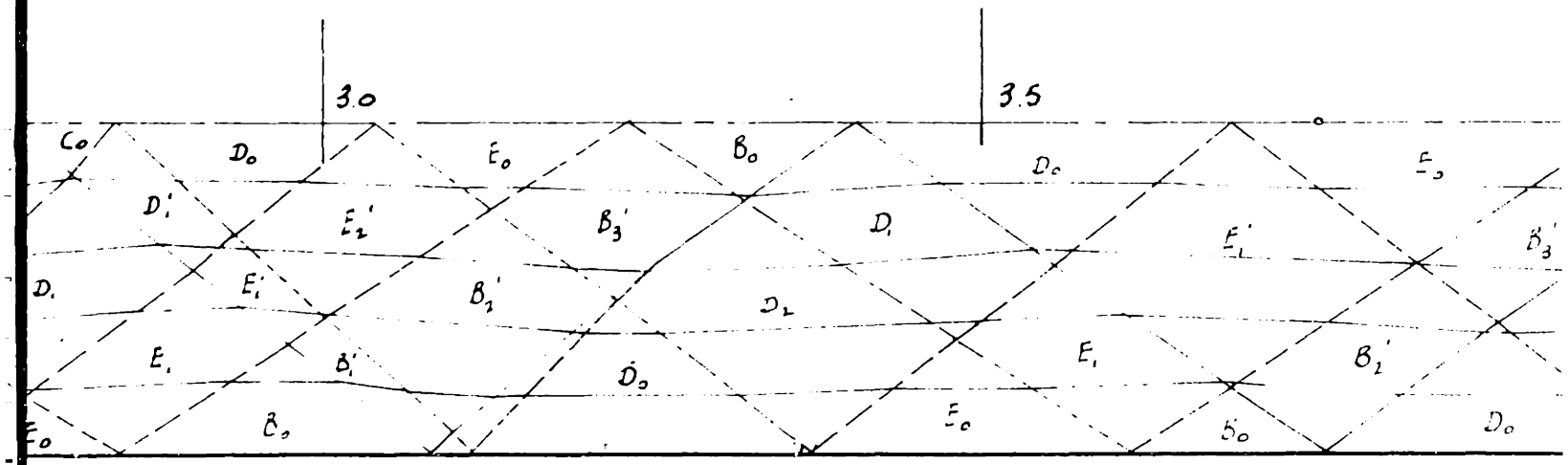

6.9°

SHARP ANG

FIEL

SHOWING STREA

FI

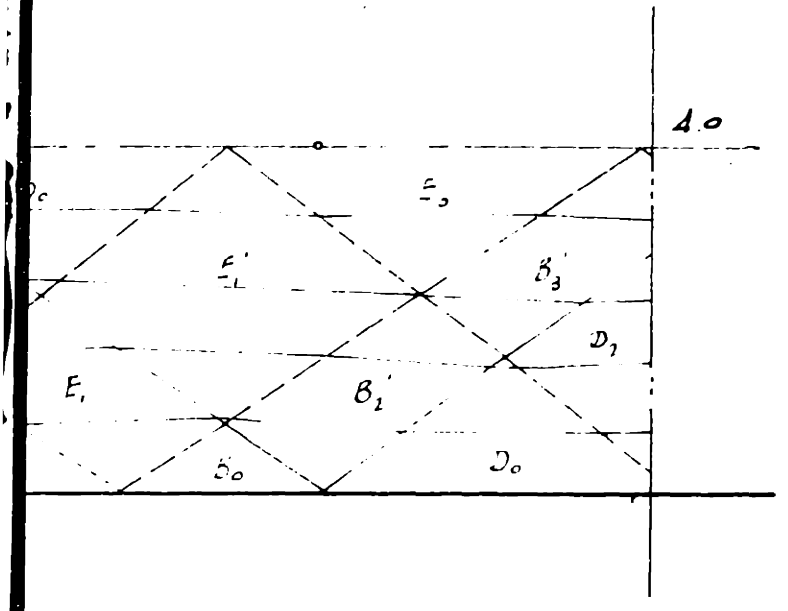

6.9° Symmetrical
Sharp Angle Contraction
Field of Flow
Showing Stream & Disturbance Lines
$F = 3.17$
FIGURE 18

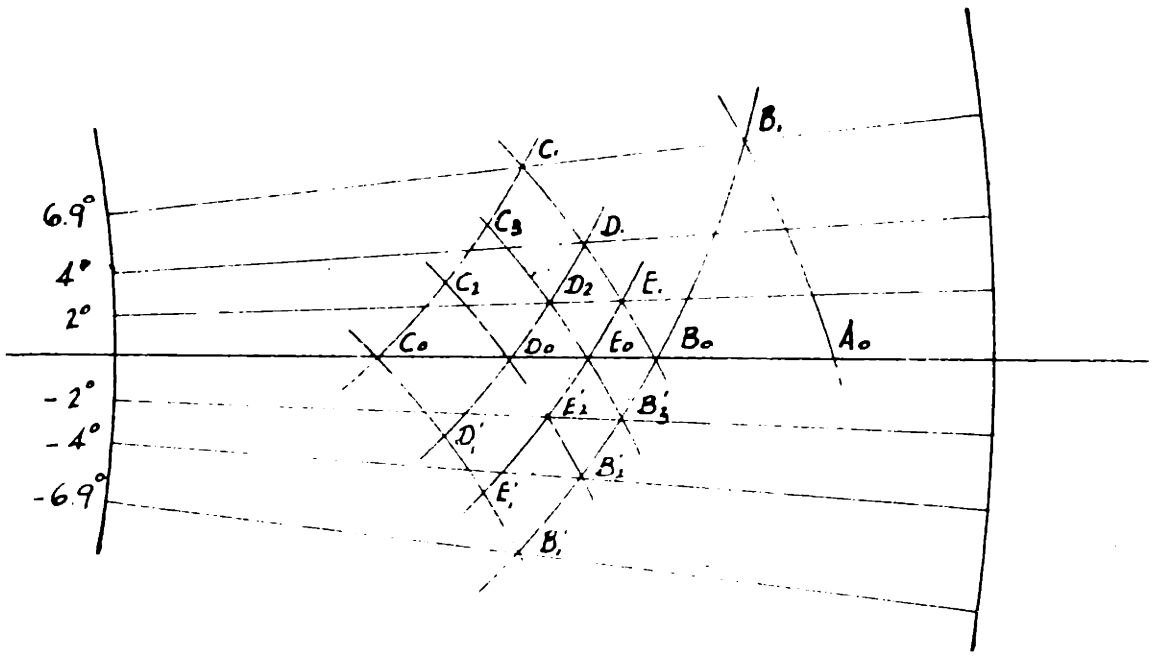

CHARACTERISTICS DIAGRAM

6.9° CONTRACTION

$\Gamma = 3.50$

FIGURE 19

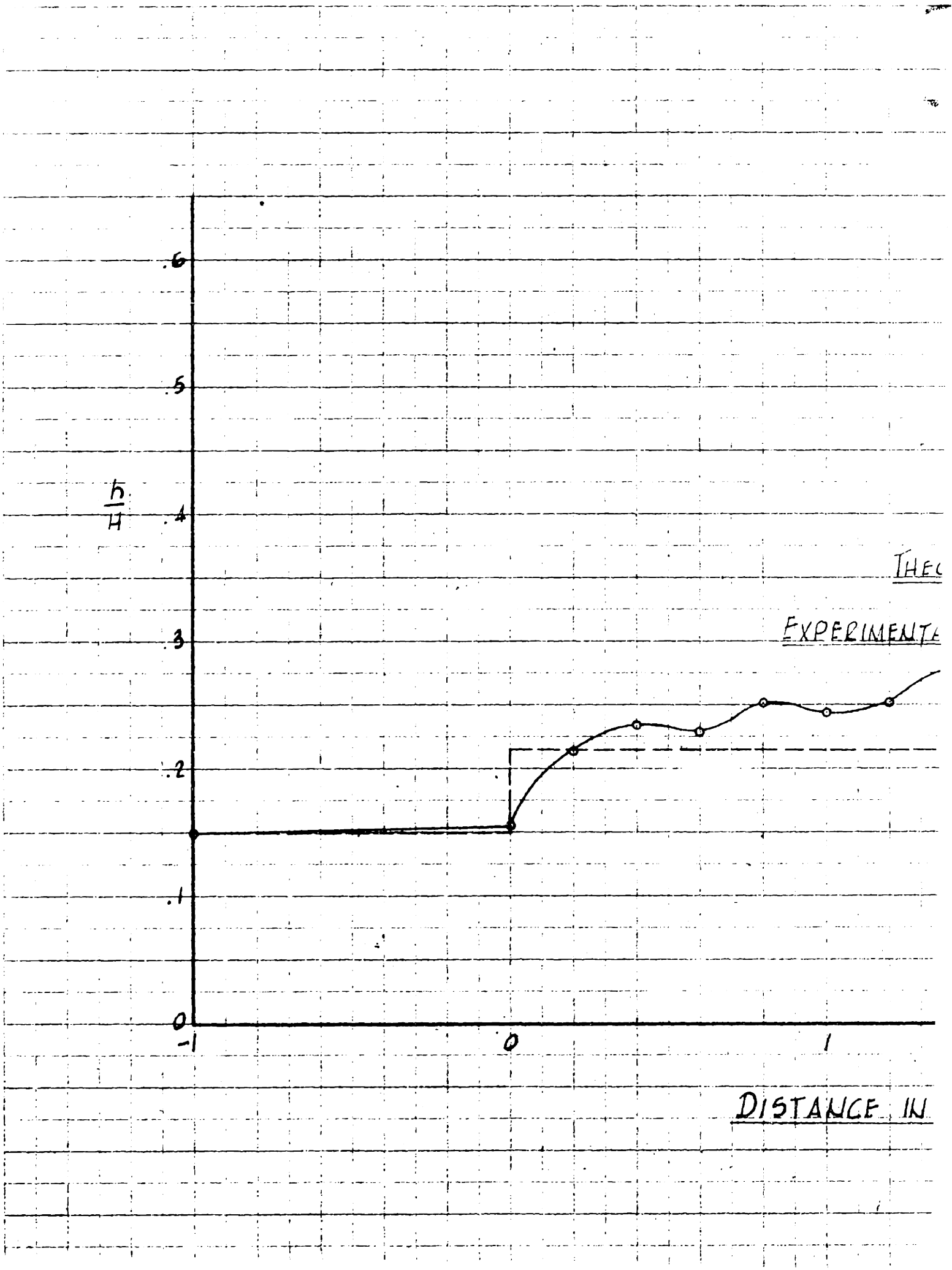
.6
.5
h/H
.4
.3
.2
.1
0
-1
0
1
THEO
EXPERIMENTA
DISTANCE IN

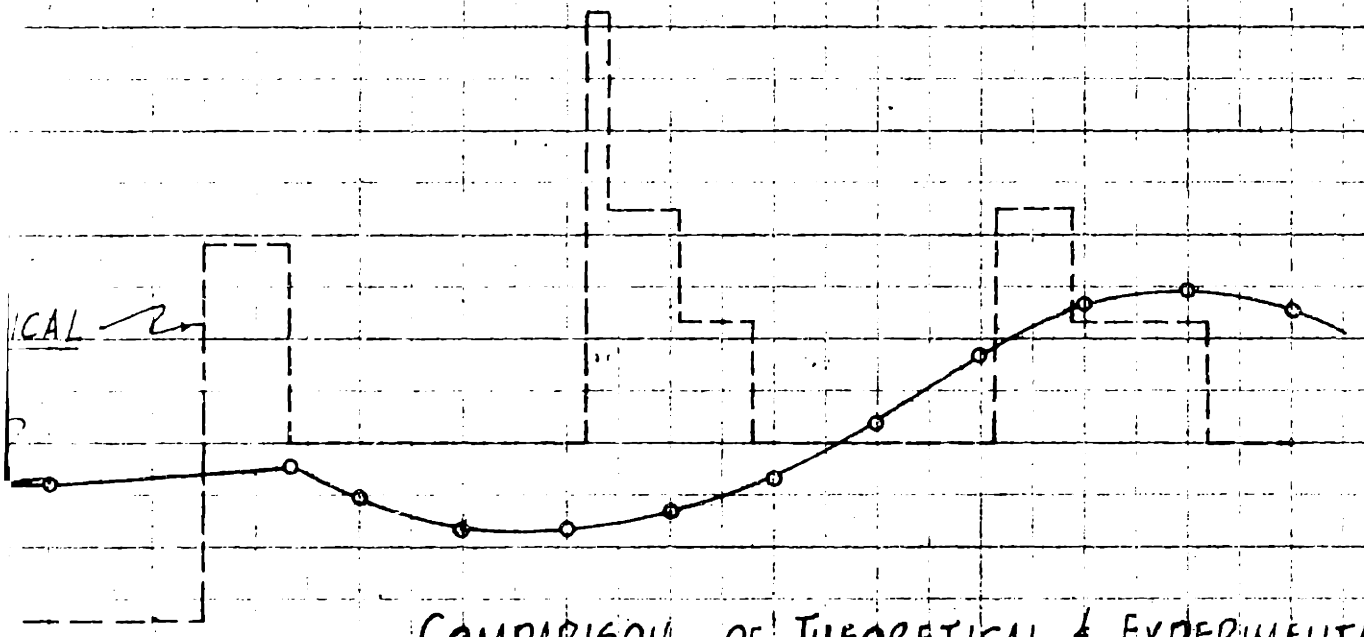

COMPARISON OF THEORETICAL & EXPERIMENTAL SIDE WALL PROFILES

6.9° CONTRACTION

F = 3.56

FIGURE 2.

2 3 4

T FROM CONTRACTION ENTRANCE

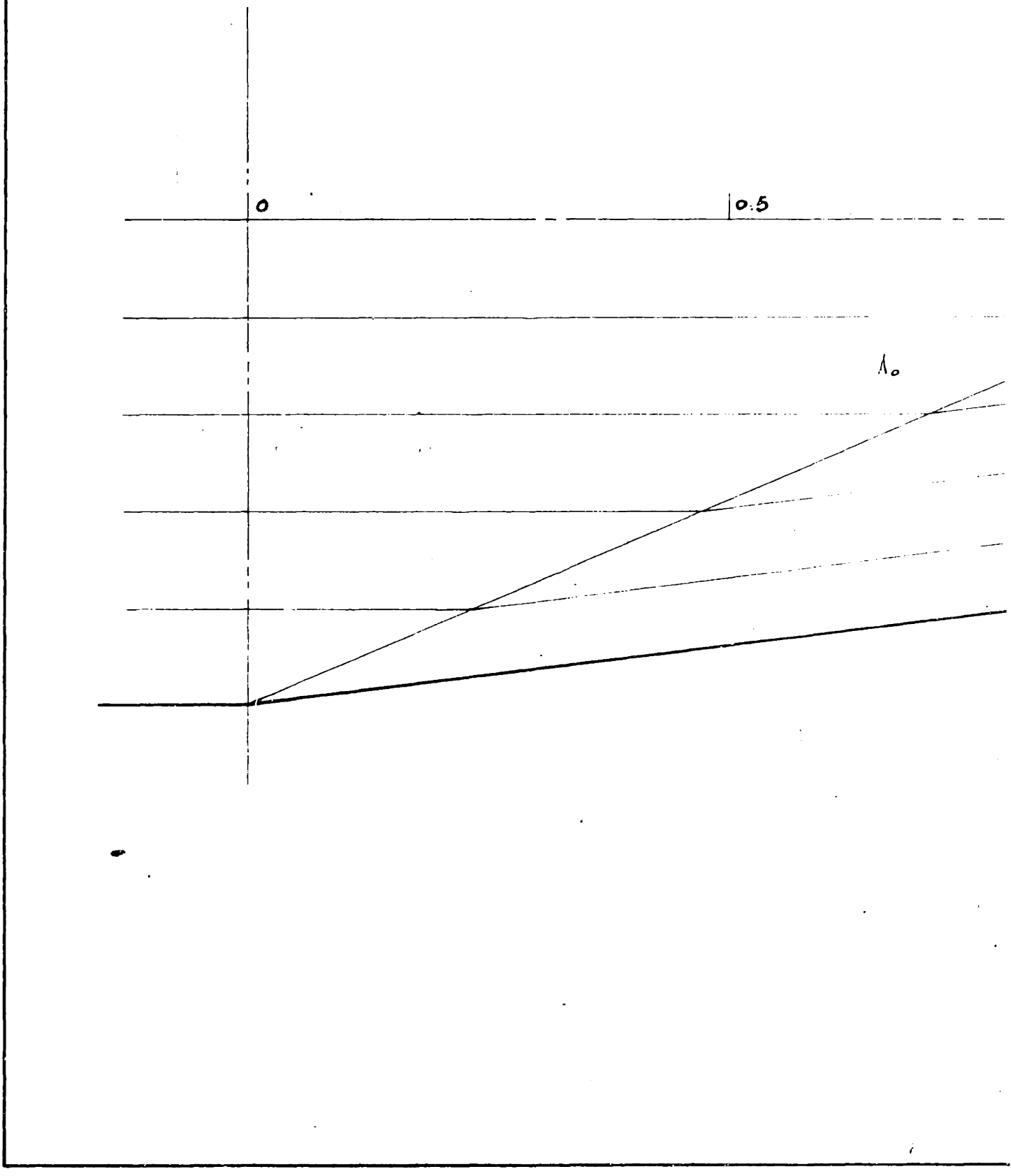
0
0.5
Λ_0

Stations Along Channel - Feet

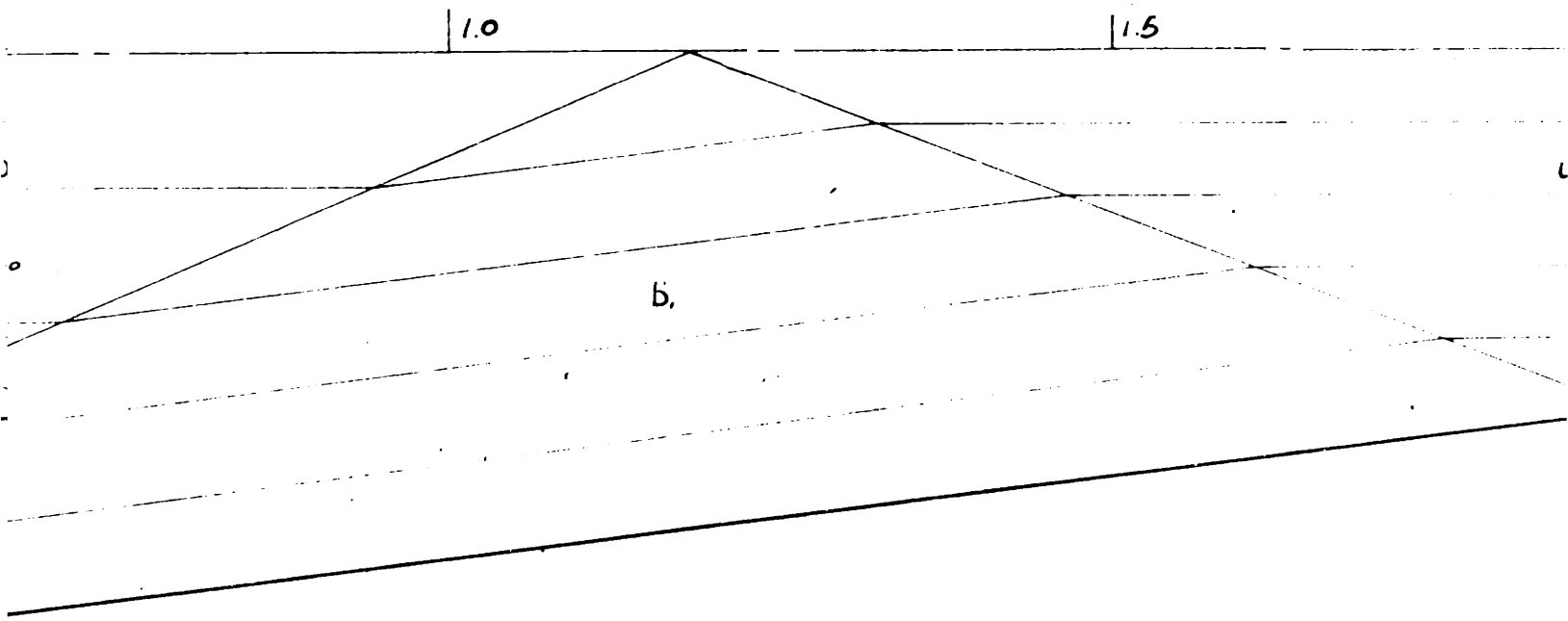

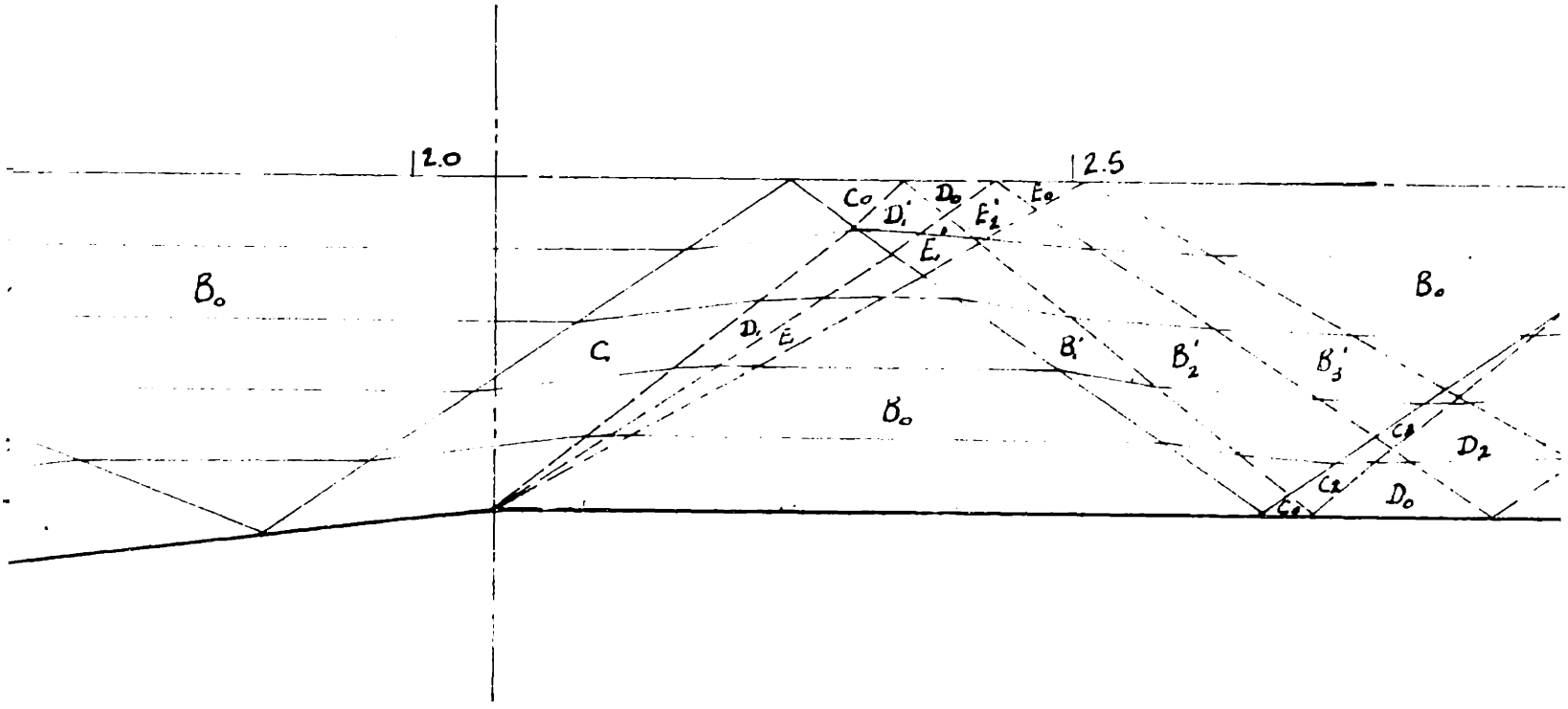
12.0
12.5
B_0
C_0
D_0
E_0
D_1'
E_1'
E_1
C
D_1
E_1
B_1'
B_2'
B_3'
B_0
B_0
C_1
D_1
C_2
D_0
C_2

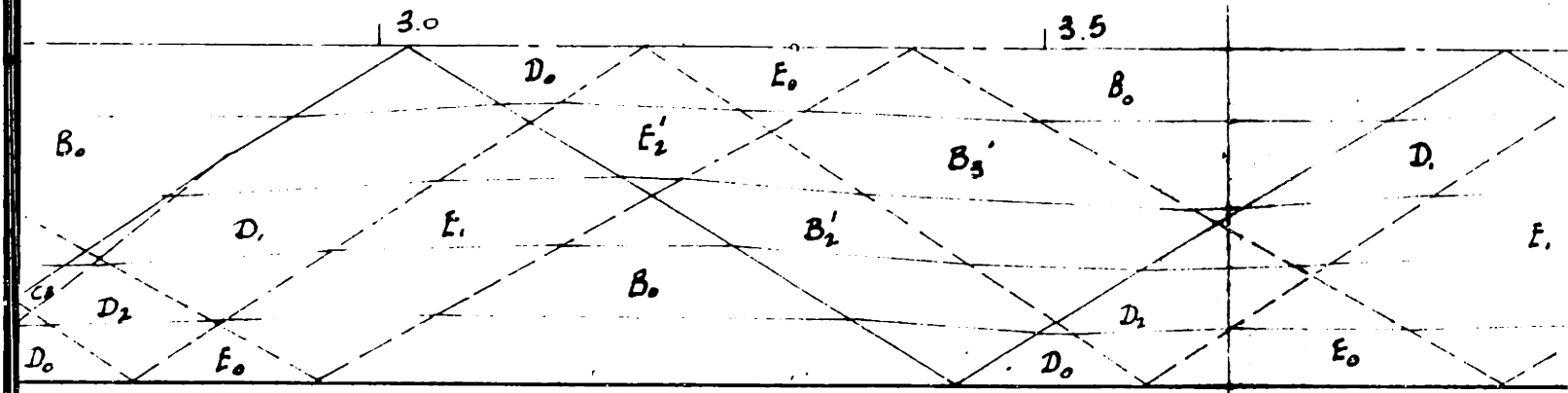

6.9° S
SHARP AN
FIELD OF
STREAM & DI
1
F

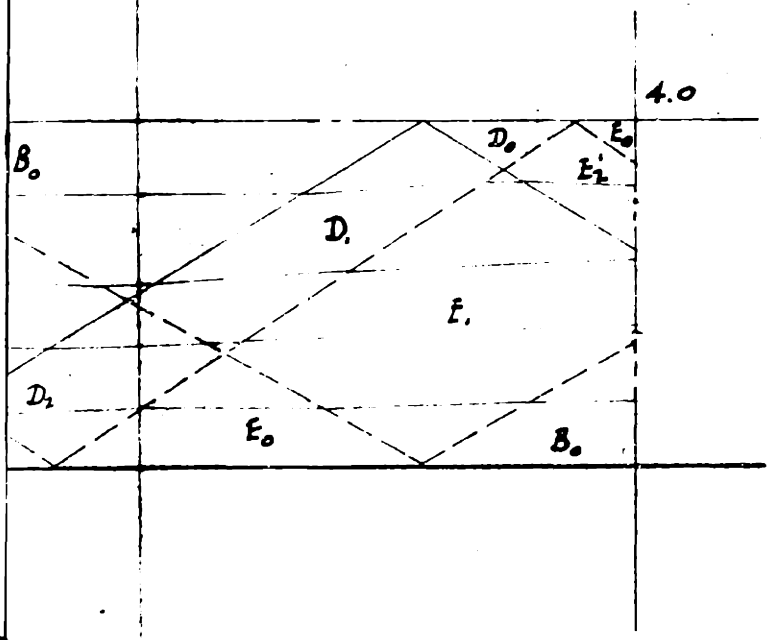

6.9° SYMMETRICAL
SHARP ANGLE CONTRACTION
FIELD OF FLOW SHOWING
STREAM & DISTURBANCE LINES
$\mathbb{F} = 3.56$
FIGURE 21

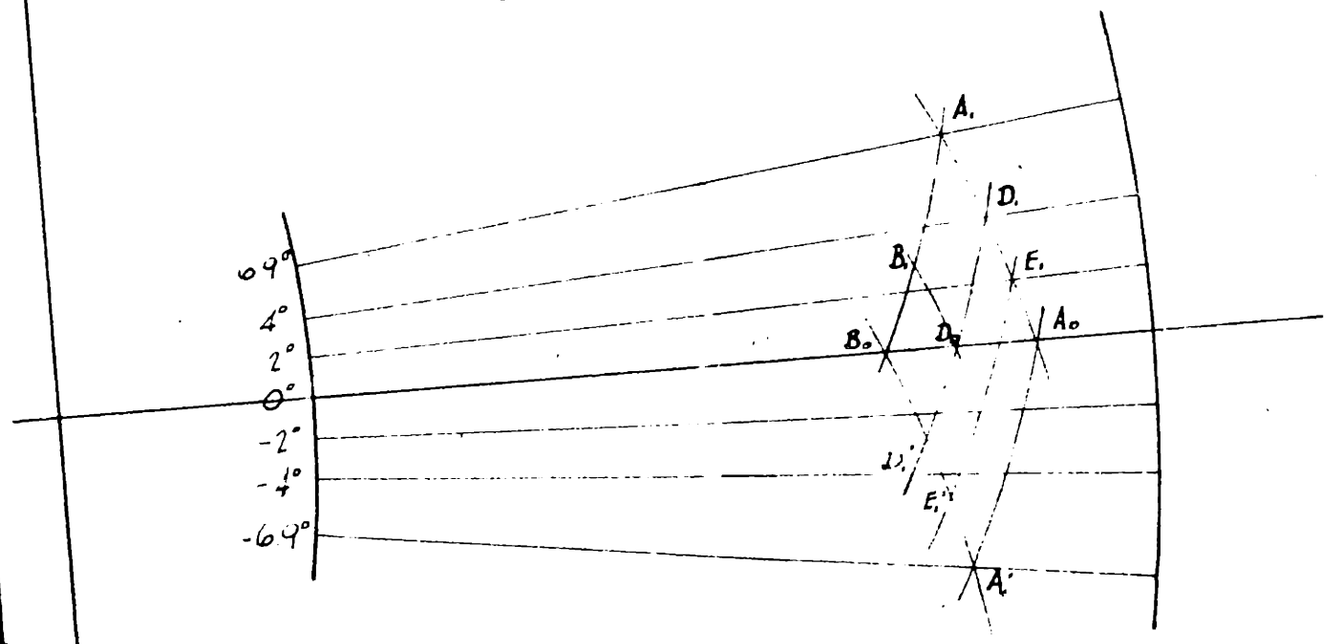

CHARACTERISTICS DIAGRAM

6.9° CONTRACTION

$\frac{F}{H} = \frac{1}{4}$

FIGURE 22

STATIONS ALON

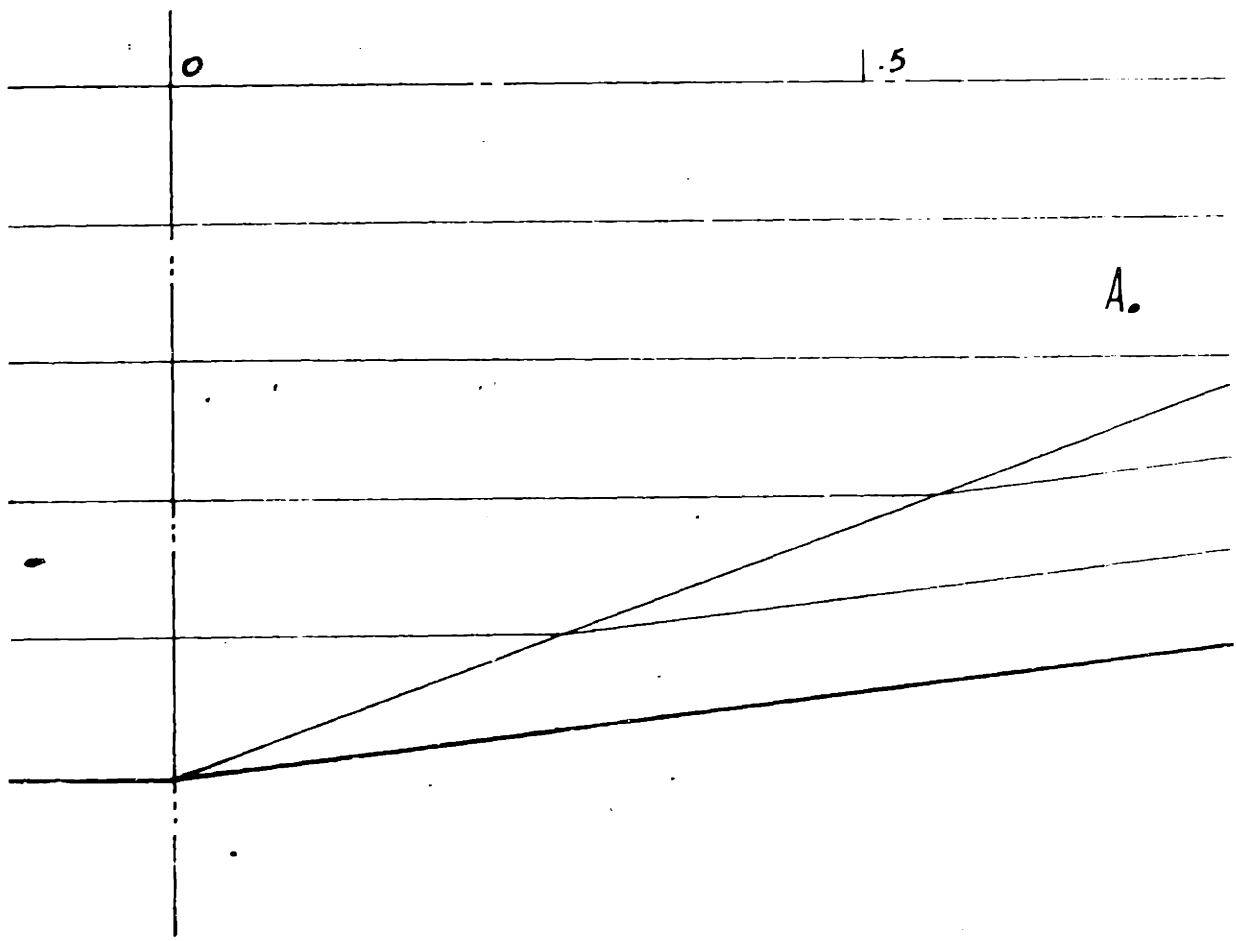

ALONG CHANNEL - FEET

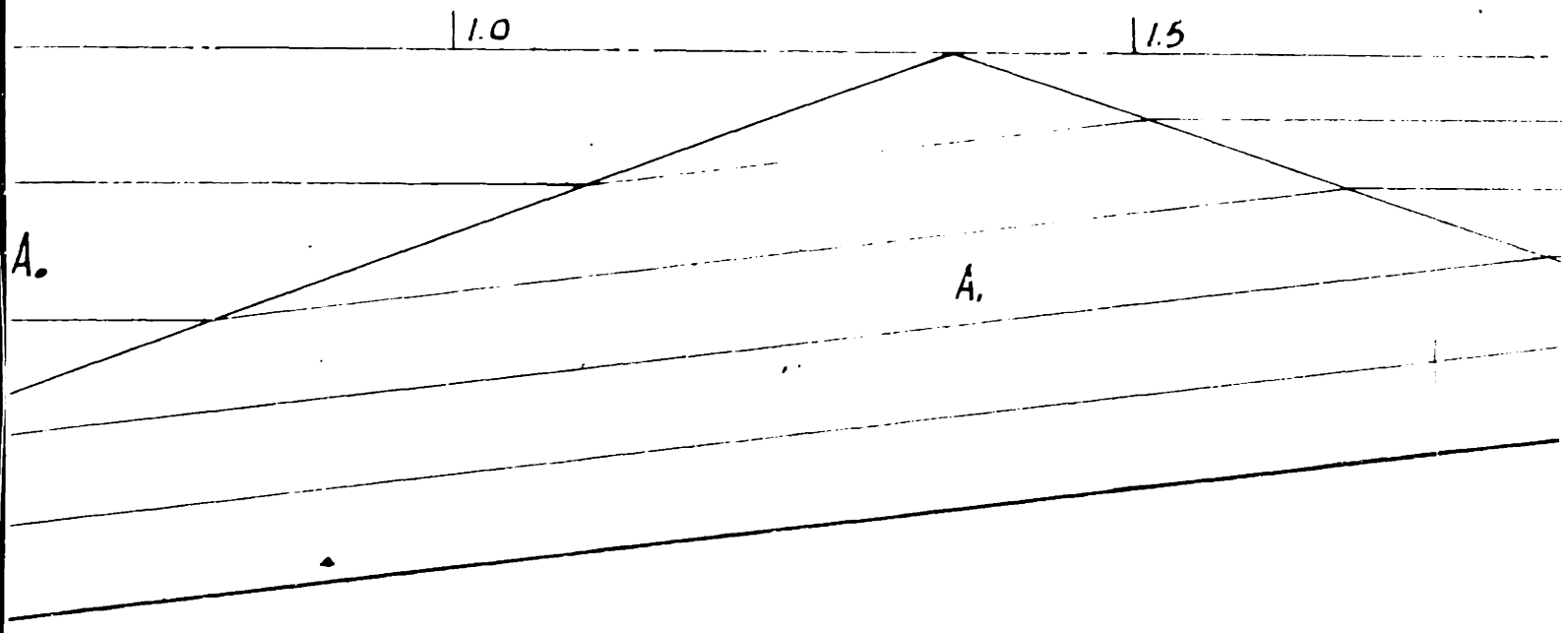

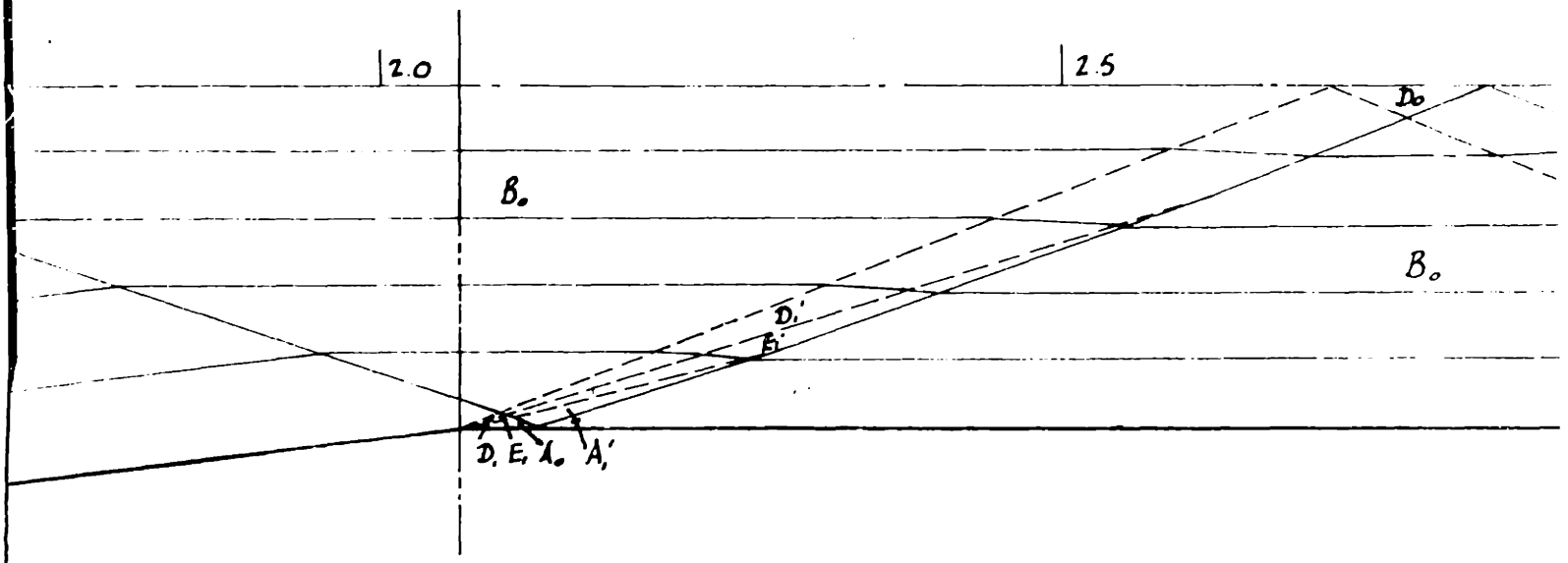
2.0
2.5
D_0
B_0
B_0
D_1'
E_1'
D, E, A_0 A_1'

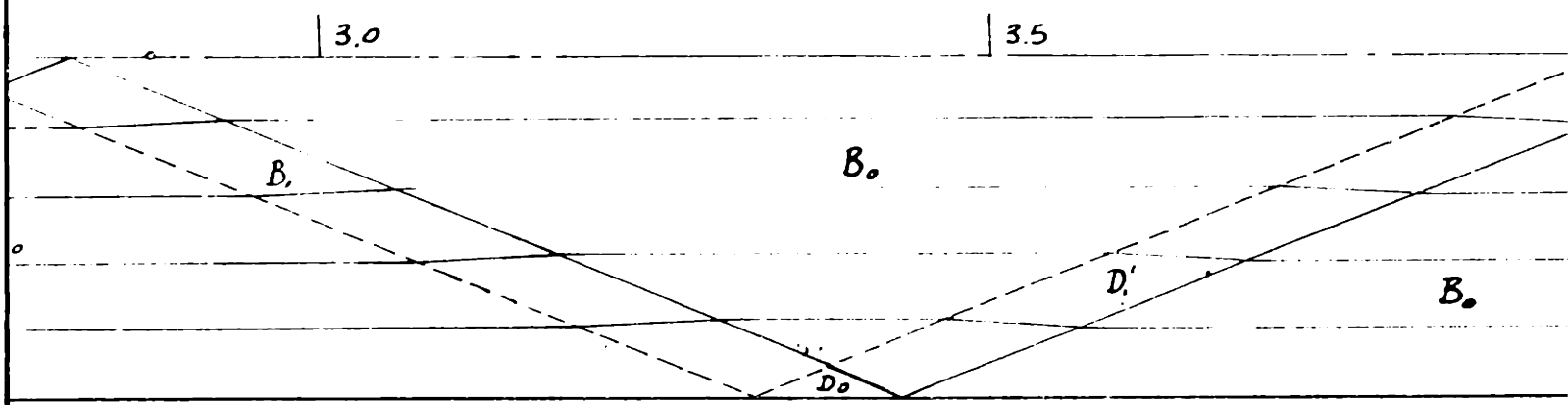

6.9° Sy
SHARP ANGL
FIELI
SHOWING STRE
I
FIG

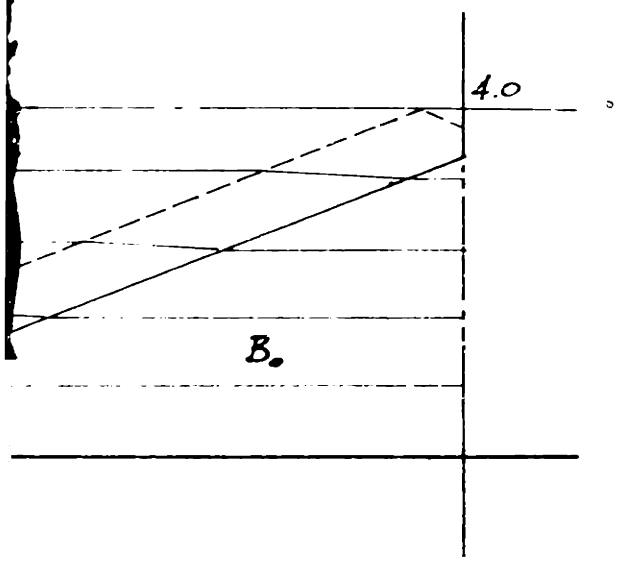

6.9° SYMMETRICAL
SHARP ANGLE CONTRACTION
FIELD OF FLOW
SHOWING STREAM & DISTURBANCE LINES
$F = 4$
FIGURE 23

APPENDIX

TABLE I

Comparison of experimental and calculated values of h_2/h_1 and β

(From work of Coles and Shintaku (8))

FROUDE NO.	h_2/h_1		β (Degrees)		
	Cal. Eq. 8	Exp.	Cal. Eq. 7	Cal. Eq. 8	Exp.
3	1.408	1.276	22.83	29.30	21.33
4	1.440	1.464	19.67	19.38	20.08
6	1.665	1.680	14.50	15.00	15.30
8	2.130	2.170	13.42	11.25	11.47
10	2.180	2.880	13.67	9.27	11.23

TABLE II

Solution of equation (14)

Information for plot of Jump Polar curves

V_{x1} = .650		V_{x1} = .675		V_{x1} = .700		V_{x1} = .725	
V_{x2}	V_y	V_{x2}	V_y	V_{x2}	V_y	V_{x2}	V_y
.620	.017	.650	.018	.650	.039	.700	.025
.600	.025	.625	.031	.600	.061	.650	.061
.580	.030	.600	.042	.550	.069	.600	.082
.560	.032	.575	.048	.525	.065	.550	.090
.540	.030	.550	.050	.500	.058	.500	.082
.520	.022	.525	.046	.475	.038	.475	.068
.508	0	.500	.033	.460	0	.450	.045
		.485	0			.436	0

V_{x1} = .750		V_{x1} = .775		V_{x1} = .800		V_{x1} = .825	
.700	.051	.750	.032	.750	.065	.800	.040
.650	.085	.700	.079	.700	.109	.700	[illegible]
.600	.105	.650	.110	.650	.138	.600	.139
.550	.112	.600	.129	.600	.155	.550	.182
.500	.106	.550	.136	.550	.162	.500	.188
.475	.096	.500	.131	.500	.157	.450	.185
.450	.079	.450	.110	.450	.139	.400	.169
.425	.050	.400	.055	.400	.100	.350	.138
.412	0	.387	0	.361	0	.335	.071
							0

TABLE II - Continued

V_{x1} = .850		V_{x1} = .875		V_{x1} = .900	
V_{x2}	V_y	V_{x2}	V_y	V_{x2}	V_y
.800	.081	.850	.051	.850	.101
.750	.134	.800	.122	.800	.165
.700	.170	.750	.174	.750	.209
.650	.196	.700	.205	.700	.231
.600	.211	.650	.228	.650	.262
.550	.217	.600	.242	.600	.275
.500	.214	.550	.247	.550	.281
.450	.197	.500	.244	.500	.278
.400	.174	.450	.232	.450	.267
.375	.153	.400	.210	.400	.247
.350	.126	.350	.171	.350	.215
.325	.081	.325	.142	.325	.192
.306	0	.300	.100	.300	.163
		.277	0	.275	.122
				.246	0

TABLE II - Continued

V_{x1} = .925		V_{x1} = .950		V_{x1} = .975	
V_{x2}	V_y	V_{x2}	V_y	V_{x2}	V_y
.900	.067	.925	.079	.950	.098
.875	.115	.900	.132	.925	.156
.850	.152	.875	.172	.900	.199
.800	.209	.850	.205	.850	.263
.750	.249	.800	.256	.800	.309
.700	.278	.700	.320	.700	.369
.600	.311	.600	.351	.600	.399
.500	.314	.500	.355	.500	.403
.400	.287	.450	.343	.400	.384
.350	.259	.400	.331	.350	.373
.300	.218	.350	.305	.300	.336
.275	.189	.300	.273	.250	.298
.250	.151	.250	.223	.225	.273
.225	.092	.225	.189	.200	.243
.212	0	.200	.143	.175	.205
		.171	0	.150	.158
				.125	.076
				.118	0

TABLE III

Values for plot of epicycloid between circles of radius $\frac{1}{\sqrt{3}}$ and 1.0

θ deg.	$\bar{V}$	θ deg.	$\bar{V}$	θ deg.	$\bar{V}$	θ deg.	$\bar{V}$
0	.577	13	.773	26	.874	39	.943
1	.613	14	.782	27	.880	40	.948
2	.635	15	.791	28	.886	41	.952
3	.651	16	.799	29	.893	42	.956
4	.666	17	.808	30	.900	43	.960
5	.683	18	.817	31	.905	44	.963
6	.695	19	.825	32	.910	45	.966
7	.709	20	.833	33	.915	46	.969
8	.720	21	.840	34	.920	47	.972
9	.731	22	.848	35	.925	48	.976
10	.742	23	.855	36	.930	49	.978
11	.753	24	.861	37	.935	50	.980
12	.763	25	.868	38	.939	65 13	1.730

DERIVATION OF RELATIONSHIP BETWEEN $\bar{V}$ AND F

By definition:

$$F = \frac{V}{\sqrt{gh}} \qquad F^2 = \frac{V^2}{gh} \qquad V^2 = ghF^2 \tag{1}$$

And again by definition:

$$\bar{V} = \frac{V}{\sqrt{2gH}} \qquad \bar{V}^2 = \frac{V^2}{2gH} \qquad V^2 = 2gH\bar{V}^2 \tag{2}$$

Combining (1) and (2):

$$ghF^2 = 2gH\bar{V}^2$$

$$\frac{h}{H} = \frac{2g\bar{V}^2}{gF^2} = \frac{2\bar{V}^2}{F^2} \tag{3}$$

From the energy equation:

$$\frac{V^2}{2g} + h = H$$

$$\frac{V^2}{2gH} + \frac{h}{H} = 1$$

$$\frac{h}{H} = 1 - \frac{V^2}{2gH} = 1 - \bar{V}^2 \tag{4}$$

Combining (3) and (4)

$$\frac{2\bar{V}^2}{F^2} = 1 - \bar{V}^2$$

$$2\bar{V}^2 - F^2 + F^2\bar{V}^2 = 0$$

$$\bar{V}^2 = \frac{F^2}{2+F^2} \qquad \bar{V} = \frac{F}{\sqrt{2+F^2}} \longleftarrow$$

This equation is plotted in the following figure.

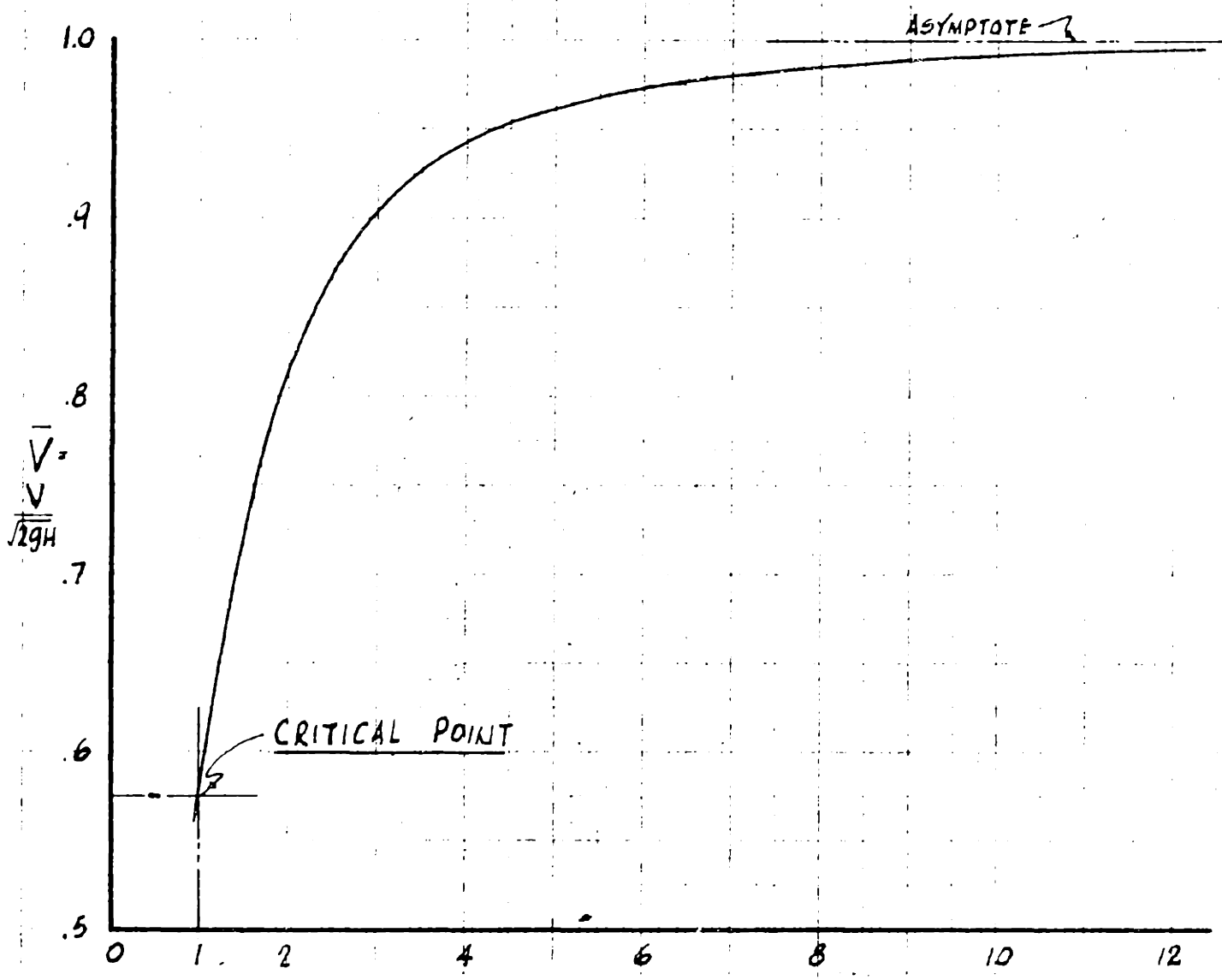

RELATION BETWEEN VELOCITY OF FLOW AND F BASED ON $\bar{V} = \frac{F}{\sqrt{1+F^2}}$

FIGURE 24

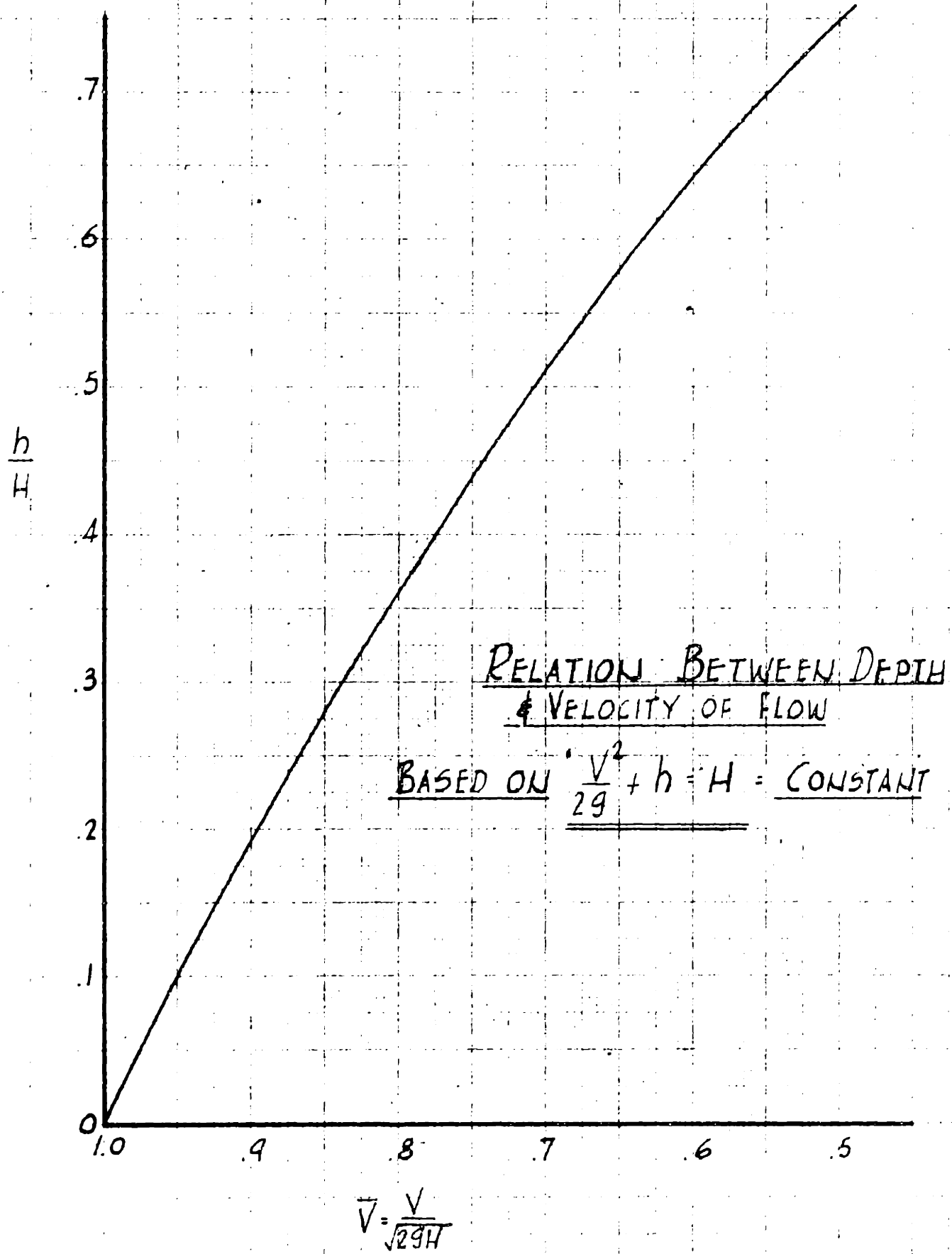

RELATION BETWEEN DEPTH & VELOCITY OF FLOW

BASED ON $\frac{V^2}{2g} + h = H = \text{CONSTANT}$

FIGURE 25

DERIVATION OF EQUATION GIVING $\frac{h}{H}$ WHEN FLOW ENTERS SUBCRITICAL RANGE

Writing the energy equation:

$$\frac{V^2}{2g} + h = H$$

Substituting $V = \frac{Q}{A} = \frac{Q}{bh}$

$$\frac{Q^2}{2gb^2h^2} + h = H$$

Multiplying by h^2 and dividing by H^3:

$$\frac{Q^2}{2gb^2H^3} + \left(\frac{h}{H}\right)^3 = \left(\frac{h}{H}\right)^2$$

$$\left(\frac{h}{H}\right)^2 - \left(\frac{h}{H}\right)^3 = \frac{Q^2}{2gb^2H^3}$$

We make the assumption of zero energy dissipation, hence H is constant, and the equation becomes:

$$\left(\frac{h}{H}\right)^2 - \left(\frac{h}{H}\right)^3 = \frac{A}{b^2} \longleftarrow$$

Where A, a constant determinable at some point in the channel where conditions are known, is given by:

$$A = \frac{Q^2}{2gH^3}$$

BIBLIOGRAPHY

(1) PRANDTL, L.,"Abriss der Stromungslehre," 1931

(2) VON KARMAN, T., "Eine praktische Anwendung der Analogie zwisbhen Ueberschallstromung in Gasen and Uberkritischer Stromung in Offenen Gerinnen," Zeitschrift fur ang. Math und Mechanik, No. 1, 1938

(3) RIABOUCHINSKY, D., "Sur l'Analogie Hydraulique des Mouvements d'un Fluide Compressible," Compt. Rend. de l'Academie des Sciences, Vol. 195, 1932, and Vol. 199, 1934

(4) BUSEMANN, A., "Gasdynamik," Handbuch der Experimentalphysik, Vol. IV, 1931

(5) PREISWERK, E.,"Application of the Methods of Gas Dynamics to Water Flows with Free Surface," Zurich Switzerland, 1938, Translation: Techn. Mem. N.A.C.A. no. 934 & 935, 1940

(6) KNAPP, R., and IPPEN, A. T., "Experimental Investigations of Flow in Curved Channels," Abstract of results and recommendations, U. S. Engineer Office, Los Angeles, Calif. 2 vols., 1938.

(7) IPPEN, A. T., "Gas Wave Analogies in Open Channel Flow," Proc. Second Hydraulics Conf., U. of Iowa, 1943

BIBLIOGRAPHY cont.

(8) DAWSON, J. H. "The effecto of lateral contractions on Supercritical flow in Open Channels," M. S. Thesis, Lehigh Uneiversity, 1943

(9) Rodriguez, D. P. "Design of a Sharp Angle Contraction in Supercritical Flow," M. S. Thesis, Lehigh University, 1943

(10) COLES, D. and SHINTAKU, T., "Experimental Relation between Sudden Wall Angle Changes and Standing Waves in Supercritical Flow." B. S. Thesis, Lehigh University, 1943